C.P. No. 1371

C.P. No. 1371

PROCUREMENT EXECUTIVE, MINISTRY OF DEFENCE

AERONAUTICAL RESEARCH COUNCIL

CURRENT PAPERS

Iterative Design Techniques for Thick Cambered Wings in Subcritical Flow

by

C. C. L. Sells

Aerodynamics Dept., R.A.E., Farnborough Hants.

LONDON: HER MAJESTY'S STATIONERY OFFICE

1977

£3 NET

UDC 533.69.01 : 533.6.04 : 533.6.044.7 : 533.6.043.1 :
533.6.043.2 : 533.6.011.32

*CP No. 1371
February 1976

ITERATIVE DESIGN TECHNIQUES FOR THICK CAMBERED WINGS IN SUBCRITICAL FLOW

by

C. C. L. Sells

SUMMARY

The author's method for computing steady, inviscid, subcritical flow past a thick cambered wing is extended to design applications. Four problems are considered: (1) given thickness and doublet (first-order loading) distributions; (2) given thickness and upper-surface pressure distributions; (3) given loading and upper-surface pressure distributions; (4) a hybrid of (2) and (3) in which the thickness is specified everywhere except near the root, and is determined near the root when the doublet distribution is constrained to exhibit spanwise invariance in that region. Convergence for the first problem is excellent. For all problems, good convergence is obtained outboard. For the single case reported of the second problem, convergence was secured near the root but cannot yet be guaranteed. Near the root, slow convergence was obtained for the third problem, rather better convergence for the fourth problem. This hybrid option is tentatively recommended.

---

* Replaces RAE Technical Report 76027 - ARC 36857.

CONTENTS

1 INTRODUCTION

This Report describes the development of computer programs to design camber and twist distributions, and in some applications thickness distributions also, for a wing without dihedral in steady inviscid incompressible (or subcritical) flow. The programs are extensions of the author's direct-calculation program, described in Ref.1, in which the flow field is represented by suitable source and doublet distributions in the wing chordal surface. A computer subroutine is available[2,3] to calculate the corresponding flow fields. Linear compressibility effects are accounted for by working in the affine (Prandtl-Glauert) space.

The design methods are based on the second-order small-perturbation theory of Weber[4]; the idea is to obtain an approximation for the planar source distribution, and the planar doublet distribution when appropriate, compute the flow fields due to these singularities, calculate the residual errors in the boundary conditions on the upper and lower surfaces, and adjust the source distribution using the symmetrical part of the error field, and the camber and twist distribution using the antisymmetrical part. Four problems are studied.

In the first problem the thickness and doublet distributions are prescribed; the doublet distribution is equivalent to the load distribution in linear theory, and is roughly equal to the difference in lower and upper surface pressure coefficients on the real, thick wing. The upper-surface (and of course the lower-surface) pressure distribution is found as part of the solution, along with the camber and twist. This method, which requires nothing beyond the suggestions of Weber[4], converges very quickly, and takes comparatively little computer time, as the velocity field on the fixed thickness surface due to the fixed doublet distribution can be calculated once for all.

In the second problem, the thickness and upper-surface pressure distributions are prescribed. The doublet strength now has to be determined iteratively. Weber has suggested[4] a procedure for this task, in which we seek to cancel the difference between the target pressure distribution and that achieved so far, by a simple addition of suitable planar doublet strength at each point, the idea being that the resulting extra streamwash will dominate. For the cases tried, this method converges quite well in mid-semispan and - perhaps surprisingly - near the tip, but near the root of a swept wing there are difficulties, in that a small change in doublet strength, particularly near the root trailing edge, does not necessarily produce a small change in the other two components,

sidewash and upwash, or in the residual error which determines the next source distribution. This leads to a situation of the tail wagging the dog. Various under-relaxation schemes have been tried, with limited success. More successful was an inner iteration scheme in which the extra sidewash and upwash due to the new doublet increments are estimated (on the chordal surface, with a direct vortex lattice representation for the upwash), the new upper-surface pressure distribution estimated and another increment in doublet strength obtained. This inner iteration has increased the scope of the method, but there are still some cases when it fails to converge, probably because for the prevailing local and temporal conditions the pressure is bounded away from the target, just as a quadratic is bounded away from certain regions. For this case an optimization routine would be appropriate, but has not been included in the program. Thus at the moment, this option cannot be guaranteed to work near the root of a swept wing.

In the third problem, the loading and upper-surface pressure distributions are prescribed, and the thickness is to be determined as well as the camber and twist. Since it is the doublet strength, and not the exact lower-surface pressure distribution, that is prescribed, this is not the same thing as the specification of both upper- and lower-surface pressure distributions, only nearly so. This time, after the computation of the first set of velocity fields, the shortfall in suction is regarded as a shortfall in streamwash due to sources, and this is turned into a perturbation thickness distribution by making use of the approximate formula of the RAE Standard Method[6] as suggested in earlier work by Weber[7]. Good convergence is achieved everywhere except near the root of a swept wing, where over-relaxation, or an inner iteration scheme similar to that described for the second problem, to take account roughly of the changes in velocity components due to the change in the thickness surface, might speed up convergence but have not been programmed.

The fourth problem is a hybrid of the second and third problems. Again the upper-surface pressure distribution is prescribed everywhere. A chordwise section, $\eta = \eta^*$ in the non-dimensional spanwise variable, is chosen near the root. Outboard of this section, the thickness distribution is prescribed, as in the second problem. This forms the basis for an iterative computation of the outboard doublet distribution. The condition is now imposed that inboard of $\eta = \eta^*$ the chordwise variation of the doublet distribution shall be the same as at $\eta = \eta^*$. In this way we expect to be able to maintain good upper surface

flow quality and wing loading right into the root, which should also be useful in obtaining root stall rather than tip stall at high off-design incidence. Finally, to secure the required upper-surface pressure distribution inboard of $\eta = \eta^*$, the thickness in that region is allowed to vary as in the third problem. At each iteration the computed thickness distribution is faired into the given outboard distribution by a least squares method; this means a certain loss of freedom, as the upper-surface pressure condition may be satisfied only in a spanwise mean sense, but it is judged important to take this precaution, in order to avoid problems in final manufacture and attachment of the wing.

As for the second problem, good convergence is found in mid-semispan and near the tip, and we can expect better convergence near the root since the difficulty associated with the second problem in that region has been bypassed. Since there is more internal freedom than in the third problem, the most we can really expect *a priori* is that convergence near the root will not be worse than for that problem, and in fact it is slightly better for the case reported here.

In our example cases for the second and third problems, the final results are noticeably different from those which we would have obtained using first-order theory, which has been the basis of classical design methods for many years, and is used here to provide first estimates with which to start the iterations. Thus, these programs should at least be useful tools for checking and refining the results of classical low-speed wing design calculations. It seems likely that the program for the fourth problem, which treats what seems to be a quite practical mixture of design conditions, will also be useful.

For the cases considered here, which are slight variations of RAE wing 'B'[8], acceptable convergence was obtained for the first problem in two or three iterations, for the second in four, for the third in five (except near the root) and for the fourth in five (including the root). Thus the second, third and fourth problems take around twice as long as the direct program[1]. This is unfortunate, and may mean that the method is less competitive than the repeated use of the BAC program[9] in an incremental mode. But there is the possibility of performing only one iteration at small cost and having a look at the results, then deciding whether to continue or to change an unpromising set of design distributions and start again, without incurring a large penalty in computer time.

Two separate programs have been written, one for the first and second problems, one for the third and fourth. The programs are written in Fortran and occupy about 45K words of core store, with arrays dimensioned for a 12 × 15 collocation grid. The vortex lattice matrix is stored on a disc.

2 BASIC EQUATIONS

In this section, we summarize the basic equations and boundary conditions as set out in detail in Ref.1.

We consider a finite wing in a uniform free stream with speed unity and Mach number $M_\infty < 1$. We take cartesian coordinates (x^*,y,z^*) with origin 0^* at the apex of the wing, with the x^*-axis 0^*x^* in the free stream direction, 0^*y to starboard and 0^*z^* upwards, $z^* = 0$ then defining the datum plane of the wing, so that at any plane station y = constant, the local wing section incidence is just the angle of twist $\alpha_T(y)$; in what follows the distribution α_T has to be determined as part of the design problem. In any plane y = constant, we define local cartesian coordinates (x,z) such that the x-axis is parallel to the local section chordline, the z-axis completes a right-handed set with the x- and y-axes, and the origin 0 is the z-projection of the apex 0^* (Fig.1). These axes can be got by rotating the (x^*,y^*)-axes through the angle $\alpha_T(y)$. Wing thickness (z_t) and camber (z_s) ordinates are defined as ordinates z_w normal to the local chord:

$$z_w(x,y) = \pm z_t(x,y) + z_s(x,y) \quad . \tag{2-1}$$

Both z_t and z_s vanish at leading and trailing edges.

The velocity in the (x,y,z) system is now made up of the free stream velocity

$$\underline{U}_\infty = (\cos \alpha_T, 0, \sin \alpha_T) \tag{2-2}$$

and a perturbation velocity field

$$\underline{u} = (u,v,w)$$

which is to satisfy the wing surface boundary condition

$$(\underline{U}_\infty + \underline{u}) \cdot \operatorname{grad}(z_w - z) = 0 \quad . \tag{2-3}$$

For compressible flow, with $M_\infty > 0$, we transform into the affine (Prandtl-Glauert, or Goethert) space $(\tilde{x},y,z)$ with the corresponding affine perturbation velocity

$$\underline{\tilde{u}} = (\tilde{u},v,w)$$

by

$$\left.\begin{aligned} x &= \tilde{x}\beta \\ u &= \tilde{u}/\beta \end{aligned}\right\} \qquad (2\text{-}4)$$

where $\beta^2 = 1 - M_\infty^2$.

To a first approximation, the problem is reduced to an incompressible flow problem in the affine space, which we proceed to tackle by placing source and doublet distributions $q(\tilde{x},y)$, $\ell(\tilde{x},y)$ on the chordal surface of the analogous wing. These distributions will generate the affine perturbation velocity field $\underline{\tilde{u}}$. We assume that at each station y = constant , $\underline{\tilde{u}}$ will not be significantly affected if the source and doublet distributions are considered as lying in the local plane $z = 0$, so that it can be calculated using the Ledger-Sells[2,3] computer subroutine.

Using this subroutine, the separate perturbation velocities $\underline{\tilde{u}}_t$, $\underline{\tilde{u}}_\ell$, due to sources and doublets respectively, will be calculated on the 'thickness surface' $z = z_t$, and their values on the actual wing surface $z = z_w$ will be derived using the first two terms of a Taylor expansion in z_s . The upwash w_t due to the sources, and the streamwash $\tilde{u}_\ell$ and sidewash v_ℓ due to the doublets, change sign on going from $z = z_t$ to $z = -z_t$, and so the components of $\underline{\tilde{u}}_t$ and $\underline{\tilde{u}}_\ell$ are:

$$\underline{\tilde{u}}_t = \left(\tilde{u}_t \pm z_s \frac{\partial \tilde{u}_t}{\partial z} , \quad v_t \pm z_s \frac{\partial v_t}{\partial z} , \quad \pm w_t + z_s \frac{\partial w_t}{\partial z}\right)$$

$$\underline{\tilde{u}}_\ell = \left(\pm \tilde{u}_\ell + z_s \frac{\partial \tilde{u}_\ell}{\partial z} , \quad \pm v_\ell + z_s \frac{\partial v_\ell}{\partial z} , \quad w_\ell \pm z_s \frac{\partial w_\ell}{\partial z}\right)$$

evaluated at $z = z_t$. Upper and lower signs correspond to upper and lower wing surfaces, respectively.

For the complete velocity $\underline{U} = \underline{U}_\infty + \underline{u}_t + \underline{u}_\ell = (U,V,W)$, making use of (2-4), we then have

$$U = \cos \alpha_T + \frac{1}{\beta}\left[\left(\tilde{u}_t + z_s \frac{\partial \tilde{u}_\ell}{\partial z}\right) \pm \left(z_s \frac{\partial \tilde{u}_t}{\partial z} + \tilde{u}_\ell\right)\right] \tag{2-5}$$

$$V = \left(v_t + z_s \frac{\partial v_\ell}{\partial z}\right) \pm \left(z_s \frac{\partial v_t}{\partial z} + v_\ell\right) \tag{2-6}$$

$$W = \sin \alpha_T + \left(z_s \frac{\partial w_t}{\partial z} + w_\ell\right) \pm \left(w_t + z_s \frac{\partial w_\ell}{\partial z}\right) . \tag{2-7}$$

These equations can now be used in the boundary condition (2-3) and will also be needed to obtain the total velocity Q from $Q^2 = U^2 + V^2 + W^2$ and the pressure coefficient C_p from

$$\left.\begin{aligned} C_p &= 1 - Q^2 \qquad (M_\infty = 0) \\ \text{or} \\ C_p &= \frac{\left[1 + \tfrac{1}{2}(\gamma - 1)M_\infty^2(1 - Q^2)\right]^{\gamma/(\gamma-1)} - 1}{\tfrac{1}{2}\gamma M_\infty^2} \qquad (M_\infty > 0) , \end{aligned}\right\} \tag{2-8}$$

where γ is the ratio of specific heats, taken here as 1.4.

Within second-order theory, for the boundary condition and for the calculation of C_p we can write $\sin \alpha_T \doteq \alpha_T$ in (2-7), and for the boundary condition (but not when calculating C_p) we can write $\cos \alpha_T \doteq 1$ in (2-5). Making these changes, we have

$$\left.\begin{aligned} U &= \tilde{Q}_0 \pm \tilde{Q}_1 \\ V &= Q_2 \pm Q_3 \\ W &= Q_5 \pm Q_4 \end{aligned}\right\} \tag{2-9}$$

with

$$\left.\begin{aligned}
\tilde{Q}_0 &= 1 + \left(\tilde{u}_t + z_s \frac{\partial \tilde{u}_\ell}{\partial z}\right)\Big/\beta \\
\tilde{Q}_1 &= \left(z_s \frac{\partial \tilde{u}_t}{\partial z} + \tilde{u}_\ell\right)\Big/\beta \\
Q_2 &= v_t + z_s \frac{\partial v_\ell}{\partial z} \\
Q_3 &= z_s \frac{\partial v_t}{\partial z} + v_\ell \\
Q_4 &= w_t + z_s \frac{\partial w_\ell}{\partial z} \\
Q_5 &= \alpha_T + z_s \frac{\partial w_t}{\partial z} + w_\ell \quad .
\end{aligned}\right\} \tag{2-10}$$

Substituting from (2-1) and (2-9) in the boundary condition (2-3), we find

$$\pm R_t + R_\ell = 0$$

whence we obtain the symmetric part of the boundary condition

$$R_t = 0 \tag{2-11}$$

and the antisymmetric part

$$R_\ell = 0 \tag{2-12}$$

where the *residuals* R_t and R_ℓ are given by

$$R_t = \frac{\tilde{Q}_0}{\beta}\frac{\partial z_t}{\partial \tilde{x}} + \frac{\tilde{Q}_1}{\beta}\frac{\partial z_s}{\partial \tilde{x}} + Q_2 \frac{\partial z_t}{\partial y} + Q_3 \frac{\partial z_s}{\partial y} - Q_4 \tag{2-13}$$

$$R_\ell = \frac{\tilde{Q}_0}{\beta}\frac{\partial z_s}{\partial \tilde{x}} + \frac{\tilde{Q}_1}{\beta}\frac{\partial z_t}{\partial \tilde{x}} + Q_2 \frac{\partial z_s}{\partial y} + Q_3 \frac{\partial z_t}{\partial y} - Q_5 \quad . \tag{2-14}$$

It is convenient here to introduce the coordinate system used for computations, which is the same as that of Ref.1. The local percentage chord is given by

$$\tilde{x} = \tilde{x}_L(y) + \tilde{c}(y)\xi \tag{2-15}$$

where $\tilde{x}_L(y)$ is the leading-edge ordinate, and $\tilde{c}(y)$ the local chord, of the analogous wing. The computation grid is then defined chordwise by equal intervals of the angular chordwise coordinate ϕ where

$$\xi = \tfrac{1}{2}(1 - \cos\phi) \quad .$$

We use the nondimensional spanwise coordinate $\eta = y/s$. (The semispan s will be taken as 1.) We also define a spanwise variable $\bar{\eta} = y$ to go with ξ , and use $\partial/\partial\bar{\eta}$ to denote partial derivative with respect to $\bar{\eta}$ along lines of constant percentage chord ξ . Then

$$\frac{\partial}{\partial\tilde{x}} = \frac{1}{\tilde{c}}\frac{\partial}{\partial\xi} \tag{2-16}$$

and

$$\frac{\partial}{\partial y} = \frac{\partial}{\partial\bar{\eta}} - \tan\tilde{\Lambda}\,\frac{\partial}{\partial\tilde{x}} \tag{2-17}$$

where $\tilde{\Lambda} = \arctan\left(\dfrac{d\tilde{x}_L}{dy} + \dfrac{d\tilde{c}}{dy}\,\xi\right)$ is the local sweep angle (for the analogous wing).

3 THE DESIGN PROBLEMS STUDIED

3.1 First problem: specified loading and thickness distributions

In this problem, the camber and twist distributions z_s, α_T are to be determined, and the upper-surface pressure distribution is found as part of the solution. We have only to determine, in addition, the auxiliary unknown source distribution, since the doublet distribution $\ell(\tilde{x},y)$ (which is equivalent to the loading distribution in linear theory) is known in advance.

Since the doublet distribution is fixed, we can compute the velocity field $\underline{\tilde{u}}_\ell$ on the thickness surface $z = z_t$ once for all. Let us assume that we have also determined an approximation $q^{(n)}(\tilde{x},y)$ to the final source distribution, and that we have computed the corresponding velocity field $\underline{\tilde{u}}_t^{(n)}$.

We suppose also that estimates for the camber distribution $z_s^{(n)}$ and twist distribution $\alpha_T^{(n)}$ are available. Using (2-13), (2-14), we compute the corresponding residuals $R_t^{(n)}$, $R_\ell^{(n)}$ and examine how well the boundary conditions (2-11), (2-12) are satisfied. Consider the first of these. The residual $R_t^{(n)}$ can be thought of as a deficiency in w_t through the term $(-Q_4)$, and so we attempt to cancel it by adding to $q^{(n)}$ a source distribution

$$\Delta q = 2R_t^{(n)} , \tag{3-1}$$

exactly as in Ref.1. To start the iteration and obtain the first estimate (the basic source distribution q_B), we take the situation where $\underline{u}_t^{(0)}$, $\underline{u}_\ell^{(0)}$ are both zero, giving the linear-theory result

$$R_t^{(0)} = \frac{1}{\beta}\frac{\partial z_t}{\partial \tilde{x}} = \frac{\partial z_t}{\partial x} ,$$

again as in Ref.1.

The residual error $R_\ell^{(n)}$ in the other boundary condition can be used to adjust the current values $z_s^{(n)}$, $\alpha_T^{(n)}$ of z_s, α_T as shown by Weber[4]. Putting

$$z_s = z_s^{(n)} + \Delta z_s , \qquad \alpha_T = \alpha_T^{(n)} + \Delta\alpha_T$$

in (2-14), neglecting products of the perturbations Δz_s, $\Delta\alpha_T$ with other perturbation quantities, and invoking (2-12), we have

$$\frac{1}{\beta}\frac{\partial \Delta z_s}{\partial \tilde{x}} - \Delta\alpha_T = - R_\ell^{(n)} . \tag{3-2}$$

To obtain the basic camber and twist distributions z_{sB}, α_{TB} with which to start the iteration, we compute $w_{\ell B}(\tilde{x},y,z_t)$ or estimate $w_{\ell B}(\tilde{x},y,0)$ from the basic doublet distribution ℓ_B, and then (2-14) gives

$$R_\ell^{(0)} = - w_{\ell B}$$

to be substituted in (3-2), which leads to the standard result of linear wing design theory.

Integrating (3-2) from 0 to ξ , using (2-16)

$$\Delta z_s(\xi;\eta) = \beta\check{c}(\eta)\left[\xi\Delta\alpha_T(\eta) - \int_0^{\xi} R_\ell^{(n)}(\xi';\eta)d\xi'\right] \tag{3-3}$$

where, since $\Delta z_s(1;\eta) = 0$, we have

$$\Delta\alpha_T(\eta) = \int_0^1 R_\ell^{(n)}(\xi';\eta)d\xi' \quad . \tag{3-4}$$

The integrals in (3-3), (3-4) are evaluated using Simpson's rule with ϕ as the independent variable. Then the accumulated z_s, α_T are extrapolated to the wing root and tip stations, and the spanwise derivative $\partial z_s/\partial\bar{\eta}$ (also needed in the Taylor series expansions) is computed at each collocation point by a cubic spline fitting routine.

We remark that the calculation of Δz_s, $\Delta\alpha_T$ does not disturb the field values $\underline{\tilde{u}}_t$, $\underline{\tilde{u}}_\ell$ on $z = z_t$, and so after finding Δz_s, $\Delta\alpha_T$ via the residual error field from Taylor series, it is worthwhile to execute the Taylor series sequence again with the updated values of z_s, α_T . This updates the successive estimates for the other residual field R_t , as well as the upper-surface pressure distribution, which we shall need in the other design problems to be considered.

3.2 Second problem: specified thickness and upper-surface pressure distributions

In this problem, the doublet distribution ℓ is to be determined iteratively, as well as the source distribution q and the camber and twist distributions z_s, α_T . A sequence of upper-surface pressure distributions $C_{pu}^{(n)}$ is generated, which (it is hoped) will tend to the specified or target distribution $\bar{C}_{pu}$. Again following Weber[4] in broad outline, successive increments $\Delta\ell$ in ℓ are determined from the shortfall in C_{pu} ; then, just as in the first problem, successive increments Δq are found from the sequence of residual errors $R_t^{(n)}$, and successive increments Δz_s, $\Delta\alpha_T$ from the sequence of residual errors $R_\ell^{(n)}$.

A first estimate ℓ_B for ℓ is provided by Lock[5]. From the target distribution $\bar{C}_{pu}$ and the appropriate equation (2-8), we derive the target upper-surface total speed distribution $\bar{Q}$, and insert it into Lock's formula:

$$D\bar{Q}^2 = \left[\cos\alpha_T + u_{tB}\cos\alpha_T + u_{\ell B}\left(1 + S^{(3)}\sec\Lambda_m^*/\beta_n\right)\right]^2$$
$$+ \left[v_{tB}\cos\alpha_T + v_{\ell B}\left(1 + S^{(3)}\sec\Lambda_m^*/\beta_n\right)\right]^2$$
$$+ \left(1 - \kappa_2^2\right)(D - 1)\sin^2\Lambda_x\cos^2\alpha_T \quad . \tag{3-5}$$

The symbols D, etc. are defined in Appendix A. The velocity components are taken in the plane $z = 0$, so that the doublet strength is connected to the (physical) component $u_{\ell B}$ by

$$\ell_B = 4\beta u_{\ell B} \quad .$$

If we tentatively assume that $v_{\ell B}$ depends linearly on $u_{\ell B}$ through a relation

$$v_{\ell B} \simeq - u_{\ell B}\tan\Lambda_v \tag{3-6}$$

where Λ_v is also defined in Appendix A, then equation (3-5) becomes a quadratic in $u_{\ell B}$ (all other quantities being known), and one of the two roots can be picked out as the required solution.

We can improve this first estimate in an iterative way, calculating v_ℓ from the current estimate for u_ℓ and the equation of irrotational flow and using this value instead of the assumption (3-6). Details are again set out in Appendix A. This is in principle an inner iteration, performed before the velocity fields $\underset{\sim}{\tilde{u}}_t^{(1)}$, $\underset{\sim}{\tilde{u}}_\ell^{(1)}$ are computed accurately in the main iteration cycle. In practice, one inner iteration is sufficient.

In an inner iteration cycle such as this, in order to estimate the successive camber and twist distributions we would like to obtain a quick estimate for the upwash corresponding to a current, or intermediate, estimate of the doublet field without performing the time-consuming Ledger-Sells double integration for each intermediate estimate in turn. To do this, we use a direct vortex lattice representation, as in Ref.1; the vortex lattice influence matrix is not inverted (but as appreciable time is needed to generate it, it is stored on a scratch disc by the computer after the first pass through the vortex lattice subroutine). Near the root and tip, the vortex lattice method is not very accurate and tends to overestimate the upwash or downwash, and so the output values are multiplied by a spanwise under-relaxation factor Ω_v tentatively taken (after numerical experiments) as:

$$\Omega_v = \frac{1}{(1 + |\kappa_2|)^2}$$

κ_2 is a spanwise interpolation function, similar to that of the RAE Standard Method, and defined in Ref.1. The errors in the resulting estimates for camber and twist will not matter greatly, since they will be nearly corrected automatically when $\underline{\tilde{u}}_\ell$ is computed accurately in the main iteration cycle.

As remarked earlier, after the calculation of $Q^{(n)}$ and $C_{pu}^{(n)}$ at the end of the nth main iteration, we have next to generate an increment $\Delta\ell$ in the doublet strength from the shortfall in C_{pu}. This shortfall is, in principle, a second-order quantity and from it, following Weber[4], we can derive a second-order expression for the corresponding increment Δu_ℓ in (physical) streamwash due to $\Delta\ell$, where as usual $\Delta\ell = 4\beta\Delta u_\ell$. Using the suffix u to represent upper-surface values in the velocity components (U,V,W) from (2-5) to (2-7), we have $Q_u^{(n)2} = U_u^2 + V_u^2 + W_u^2$, and to second-order accuracy

$$\bar{Q}^2 \doteq (U_u + \Delta u_\ell)^2 + V_u^2 + W_u^2$$

$$\doteq Q_u^{(n)2} + 2U_u\Delta u_\ell$$

whence

$$\Delta u_\ell = \frac{\bar{Q}^2 - Q_u^{(n)2}}{2U_u} \quad . \tag{3-7}$$

We now have all the equations needed to set up a closed iteration cycle for this problem.

In order to control some overshoot near the tip (and as a partial control near the root also - this will be discussed further, later), it has been found helpful to introduce an under-relaxation factor Ω_D for the doublet strength perturbations, again depending on the spanwise factor κ_2 :

$$\Omega_D = (1 + |\kappa_2|)^{-\frac{1}{2}} \quad .$$

Near a wing tip of finite chord, the loading is expected (apart from the effect of corner singularities) to decay elliptically; the factor Ω_D is not expected to represent this spanwise decay precisely, but is intended to introduce some decay, under control, which seems in practice to be better than introducing none at all.

It will be remembered[1] that, to assist the solution of the direct problem, line source and doublet distributions were introduced on the wing centre line $y = z = 0$ to reduce the residual errors R_t, R_ℓ at the root $y = 0$. In the present design problem, just as we adjust the planar doublet strength to produce an extra Δu_ℓ to correct the upper-surface pressure distribution outboard, it is natural to try to adjust the line doublet strength to produce an extra streamwash $\Delta u_{\ell D}$ to do the same job at the root. The resulting upwash adjustment $\Delta w_{\ell D}$ would then be incorporated into the camber and twist distribution at and near the root. The difficulty is, that whereas (in the direct problem) a change in line doublet strength to produce a certain $\Delta w_{\ell D}$ did not tend to produce a large change $\Delta u_{\ell D}$, a change to produce a certain $\Delta u_{\ell D}$ does tend to produce a large change $\Delta w_{\ell D}$; in other words, this calculation, although well-conditioned in one direction, is ill-conditioned in the other. It was found that line sources also tended to destabilize the iteration scheme; so the line singularity technique has been abandoned and no target distribution is prescribed at the wing root (though we can approach it quite closely with a suitable choice of spanwise stations); all quantities such as z_s, q, ℓ are extrapolated parabolically to the root (but $\underline{\tilde{u}}_t$, $\underline{\tilde{u}}_\ell$ are still evaluated using the Ledger-Sells subroutine), and the final residual errors and pressure coefficients at the root are left to take care of themselves.

As in the direct program[1], we can seek to reduce the number of iterations by generating improved estimates for the perturbation quantities. The additional velocity fields due to the perturbation source and doublet fields, calculated in the main iteration cycle, can be estimated using the RAE Standard Method[6] and so it is possible in effect to perform one iteration cycle and to obtain a further set of perturbation quantities, without actually performing the accurate but lengthy Ledger-Sells calculations. To estimate the new residual errors, we again invoke Maclaurin series (expansions about $z = 0$, rather than $z = z_t$), modified to take account of concurrent changes in camber. The algebra is set out in Appendix B. This can indeed be incorporated in a further inner iteration cycle, but it has been found inadvisable to do it more than once or twice; convergence of the main iteration cycle is rather sensitive, perhaps because of the level of feedback involved between the three unknown and interacting field quantities, and it seems likely that any further benefit derived after the first or second inner iteration is outweighed by the feedback effect due to the accumulating errors in the successive estimates from each cycle.

In the course of developing the program, a difficulty has arisen which has still not been satisfactorily resolved. The symptom of this difficulty is the onset of oscillations or divergence in v_ℓ, w_ℓ, C_{pu} and R_t near the root trailing edge. In this region there seems to be a close coupling between all the velocity components so that a small change in ℓ and hence in $\tilde{u}_\ell$ does not necessarily produce a negligible change in v_ℓ, w_ℓ and in the residual error R_t ; thus the effect of the small change $\Delta\ell$ given by (3-7) does not have the required effect on Q_u .

To prevent R_t and the resulting extra source distributions from growing too large, after the first guesses for source and doublet fields the program has been arranged to do two successive perturbation source calculations (including Maclaurin series calculations), just as if it were performing two iterations of the first problem, before calculating another perturbation doublet field. This is an unfortunate necessity, but as the Ledger-Sells subroutine is adaptive, the calculation times should decrease as the iterations proceed and R_t decreases.

The destabilizing effect of Δv_ℓ and Δw_ℓ is not so easily dealt with. An attempt to take them into account in the derivation of equation (3-7), even when only linear terms are included, leads to some heavy matrix algebra and programming, and fails in the end because the non-linear terms are not negligible in practice. For some of the cases studied, instability was successfully averted by a simple addition to the inner iteration scheme, in which we take account of the approximate values of $\Delta\tilde{u}_\ell$, Δv_ℓ, Δw_ℓ (and also of $\Delta\tilde{u}_t$, Δv_t, Δw_t generated within the Maclaurin series sequence, when appropriate) to update approximately the upper-surface velocity components U_u, V_u, W_u and the total speed Q_u and hence to generate a further perturbation doublet field using (3-7) again. This part of the inner iteration cycle can now be repeated until the changes in doublet strength are sufficiently small, or for a maximum of (currently) nine inner cycles. This inner iteration scheme can also be profitably applied to the rest of the wing surface, even though the effect of Δv_ℓ and Δw_ℓ on Q_u is not so great.

This artifice has enabled us to obtain a solution for at least one case which we could not treat without it. But there seems to be a class of cases for which the program so far described still does not work; for these cases, it is the inner iteration which oscillates or diverges. Relaxation methods do not seem to help. A study of the computer output indicates that, even though a numerically exact solution of the whole problem is known (derived from the program for the first problem, for instance), the unconverged state of the

accurately calculated parts of $\underline{\tilde{u}}_t$ and $\underline{\tilde{u}}_\ell$, and the approximations used for $\Delta\underline{\tilde{u}}_\ell$ in terms of $\Delta\ell$ in the inner iteration scheme, are such that Q_u has a minimum value which is higher than the design value $\bar{Q}$, just as a quadratic in a real variable is bounded away from certain values. Thus in this situation we cannot find a $\Delta\ell$ to give $Q_u = \bar{Q}$ everywhere, using just the inner iteration scheme. An optimization sequence within this scheme, to detect the situation and to seek a solution minimizing the overall differences between Q_u and $\bar{Q}$ (by least squares, perhaps) is indicated, but has not been devised at the time of writing.

3.3 Third problem: specified loading and upper-surface pressure distributions

In this problem, the thickness distribution z_t is to be determined iteratively, as well as the camber and twist distributions z_s, α_T and the associated source distribution q. Again a sequence of upper-surface pressure distributions $C_{pu}^{(n)}$ is generated, which (it is hoped) will tend to the target distribution $\bar{C}_{pu}$.

As in the first and second problems, successive source increments Δq are found from the sequence of residual errors $R_t^{(n)}$, and successive camber and twist increments Δz_s, $\Delta\alpha_T$ from the sequence of residual errors $R_\ell^{(n)}$. This leaves the successive thickness increments Δz_t to be determined from the shortfall in upper-surface C_{pu}. We can do this approximately, making use of results from the RAE Standard Method[6], if this shortfall can be converted approximately into a shortfall $\Delta\tilde{u}_t$ in $\tilde{u}_t$. We may consider the following three sets of circumstances:

(i) At the outset, we have no estimate at all for z_t. Given the design upper-surface velocity $\bar{Q}_u$ and the chordal-surface streamwash $\tilde{u}_{\ell B}$ due to the specified load (doublet) distribution, we have a simple basic estimate for the streamwash due to sources:

$$\tilde{u}_{tB} = \beta(\bar{Q}_u - 1) - \tilde{u}_{\ell B} \quad .$$

This will lead to a first estimate z_{tB} for the thickness distribution.

(ii) We can modify this initial crude estimate for z_t with the help of Lock's formula (3-5). From the known doublet strength, we again have $\tilde{u}_{\ell B}$ (hence $u_{\ell B}$) and also $v_{\ell B}$, on the chordal surface. If we assume that u_{tB}, in the first term on the right side of (3-5), dominates the equation as far as sources are concerned, we can substitute for all the other source terms, such as

v_{tB} , the values determined from the initial estimate z_{tB} and obtain a revised estimate for $\tilde{u}_t$ (and hence a revised estimate for z_t). The details are filled in at the end of Appendix A.

(iii) After computing $C_{pu}^{(n)}$ in the nth main iteration, just as in the second problem we can derive a simple second-order expression for the required physical increment $\Delta u_t = \Delta\tilde{u}_t/\beta$ due to the required extra thickness distribution Δz_t . This expression is just the right side of equation (3-7) again:

$$\Delta u_t = \left[\bar{Q}^2 - Q_u^{(n)2}\right] \Big/ 2U_u \quad .$$

After a Maclaurin series cycle, the velocity components in this expression can be approximately updated, as in the second problem.

The perturbation velocity $\Delta\tilde{u}_t$ and the extra thickness Δz_t (which can be thought of as an extra source distribution $2\partial\Delta z_t/\partial\tilde{x}$) are connected approximately by the formula of the RAE Standard Method[6]:

$$\Delta\tilde{u}_t = \cos\tilde{\Lambda}\left[\sigma\left(\frac{\partial\Delta z_t}{\partial\tilde{x}}\right) - \kappa_2(\eta) f(\tilde{\Lambda}) \frac{\partial\Delta z_t/\partial\tilde{x}}{\sqrt{1 + (\partial\Delta z_t/\partial\tilde{x})^2}}\right]$$

with

$$\sigma = \frac{1}{\pi}\int_0^1 \left(\frac{\partial\Delta z_t}{\partial\tilde{x}}\right)_{\xi'} \frac{d\xi'}{\xi - \xi'} \qquad (3\text{-}8)$$

$$f = \frac{1}{\pi} \ln \frac{1 + \sin\tilde{\Lambda}}{1 + \sin\tilde{\Lambda}} \quad .$$

κ_2 is the spanwise interpolation function, defined in Ref.1. One way of dealing with this equation is to set up an iterative cycle in which the last term (with 'Riegels factor') is treated as small and known from the previous iteration - indeed, it vanishes altogether at certain mid-wing stations where $\kappa_2 = 0$. Thus we write

$$\sigma\left(\frac{\partial\Delta z_t^{(m)}}{\partial\tilde{x}}\right) = \frac{\Delta\tilde{u}_t}{\cos\tilde{\Lambda}} + \kappa_2 f(\tilde{\Lambda}) \frac{\partial\Delta z_t^{(m-1)}\big/\partial\tilde{x}}{\sqrt{1 + \left(\partial\Delta z_t^{(m-1)}\big/\partial\tilde{x}\right)^2}} \equiv F \qquad (3\text{-}9)$$

at the mth such cycle, and to start the cycle we put $\Delta z_t^{(0)} = 0$. The solution of this equation (see Ref.7, for example) with $\Delta z_t^{(m)}(1) = \Delta z_t^{(m)}(0) = 0$ is:

$$\frac{\partial \Delta z_t^{(m)}}{\partial \tilde{x}} = -\frac{1}{\sqrt{\xi(1-\xi)}} \frac{1}{\pi} \int_0^1 F(\xi') \sqrt{\xi'(1-\xi')} \frac{d\xi'}{\xi - \xi'} \quad . \tag{3-10}$$

The program already incorporates a subroutine to evaluate the Cauchy (principal-value) integral (3-8), and the Cauchy integral (3-10) can be evaluated using the same subroutine; thus the method is more convenient than, for example, an extension of Carleman's method as in Ref.7.

However, before actually coding the evaluation of (3-10) we should consider that the initial guess z_{tB}, and the corrections Δz_t, should represent a wedge-shaped trailing-edge ($\xi = 1$) for structural reasons; whereas, if F is assumed regular at $\xi = 1$, then $\partial \Delta z_t / \partial \tilde{x}$ is $0\left[(1-\xi)^{-\frac{1}{2}}\right]$ and Δz_t takes a rounded or elliptical shape there, as well as at the leading-edge $\xi = 0$. On the other hand, when Δz_t is regular, σ and F will show a logarithmic singularity as $\xi \to 1$. We therefore estimate the strength of the singularity and subtract a suitable function from F to leave an integrand which we hope will lead to a sensible trailing-edge shape.

A representative function Δ_0 which represents a closed section, with a suitably small square-root singularity at the leading-edge and wedge-shaped at the trailing-edge, is

$$\frac{\partial z_{t0}}{\partial \tilde{x}} = \Delta_0 = \tfrac{1}{2}(3 - 5\xi)\sqrt{\xi} \tag{3-11}$$

which corresponds to a section shape

$$z_{t0}/\tilde{c} = (1-\xi)\xi^{3/2} \quad .$$

Inserting (3-11) in (3-8), we have

$$\sigma_0 = \frac{1}{\pi}\left[\frac{5}{3} + (3 - 5\xi)\left(\frac{1}{2}\sqrt{\xi}\,\ln\frac{1+\sqrt{\xi}}{1-\sqrt{\xi}} - 1\right)\right] \quad .$$

We now subtract a suitable multiple δ of σ_0 from F. To help determine this multiple, we have the values of F at discrete chordwise stations $\xi_2, \xi_3, \ldots, \xi_{L-1}, \xi_L$ where $0 = \xi_1 < \xi_2 < \ldots < \xi_L < 1$. We make the hypothesis

$$F = \delta\sigma_0(\xi) + \sigma_1(\xi)$$

where $\sigma_1(\xi)$ varies slowly compared with $\sigma_0(\xi)$ near $\xi = 1$. Putting $\xi = \xi_{L-1}$, ξ_L in turn and subtracting, we find

$$\delta \doteq \frac{F(\xi_L) - F(\xi_{L-1})}{\sigma_0(\xi_L) - \sigma_0(\xi_{L-1})} .$$

We then evaluate Δ^* from the equation, similar to (3-10)

$$\Delta^* = -\frac{1}{\sqrt{\xi(1-\xi)}} \frac{1}{\pi} \int_0^1 \left[F(\xi') - \delta\sigma_0(\xi')\right] \sqrt{\xi'(1-\xi')} \frac{d\xi'}{\xi - \xi'}$$

and then

$$\frac{\partial \Delta z_t^{(m)}}{\partial \bar{x}} = \Delta^* + \delta\Delta_0 .$$

This can now be substituted into F given by (3-9), with m increased by one, to start the next iteration cycle. We have tested this cycle on a variety of wings and shapes, and convergence always seems rapid, up to 10 iterations being needed depending on the value of the interpolation function κ_2.

Although the integral (3-10) and the function (3-11) always represent closed contours mathematically, when $\Delta z_t^{(m)}$ is evaluated by numerical integration of $\partial \Delta z_t^{(m)} / \partial \bar{x}$ this may not be exactly true because of numerical truncation errors. At each cycle, then, we check the closure condition and rotate the contour $\Delta z_t^{(m)}$ through a small correction angle about the leading-edge in the $(\xi, \Delta z_t)$ plane to make $\Delta z_t^{(m)} = 0$ at $\xi = 1$.

After calculating Δz_t we must check that the resulting contour does not cross itself, i.e. the new z_t is positive everywhere. Actually, we demand rather more. To avoid the possibility of unrealistically small z_t, we check that z_t will not be reduced by more than half its former value anywhere; if this condition is not met, i.e. $\Delta z_t < -\frac{1}{2} z_t$, then Δz_t is everywhere multiplied by a suitable factor to give just the 50 per cent reduction in z_t at some point which is the largest reduction we are prepared to allow.

On the other hand, if the first estimate z_{tB} fails this test, since there is no previous distribution to compare it with, we have to improvise. First, we examine z_{tB} near the leading edge; if it is negative somewhere in that region, then probably the input data for ℓ and C_{pu} do not correspond to a reasonable wing; the program exits. If z_{tB} is positive there, but becomes negative near the wing trailing-edge, we charitably assume that the input data do correspond to a reasonable wing and the initial guess for z_{tB} is in error. At each spanwise station we then find the maximum z_{tB}, at $\xi = \hat{\xi}$ say, and also note the derivative $\partial z_{tB}/\partial\xi$ at $\hat{\xi}$. For $\hat{\xi} \leqslant \xi \leqslant 1$ we construct a function $G(\xi)$ which is arcwise continuous with z_{tB} at $\xi = \hat{\xi}$, becomes rapidly linear as we recede from that point, and vanishes at the trailing-edge $\xi = 1$. A suitable function is

$$G = ae^{-k(\xi-\hat{\xi})} + b\xi + c$$

where we arbitrarily choose k so that

$$k(1 - \hat{\xi}) = 2$$

so that the exponential term dies out near $\xi = 1$. a, b and c can now be chosen to meet the three conditions (Appendix C).

We apply this procedure at all spanwise stations, even if a negative z_{tB} has been detected at only one station, because $\partial z_{tB}/\partial y$ (which is needed for the boundary conditions) has to be computed from the values generated, and if we only adjusted the values at one such station, the difference between the adjusted section and the neighbouring unadjusted sections downstream of $\xi = \hat{\xi}$ might cause considerable fluctuations in this spanwise derivative. By applying the procedure uniformly at all spanwise stations, we hope to avoid this possible source of trouble.

Indeed, each time a fresh z_t is computed for this problem, we have to compute and store the new chordwise derivative $\partial z_t/\partial\xi$ as well as $\partial z_t/\partial y$, and we also need[1] the tables of arclengths along chordwise and spanwise curves on the new thickness surface $z = z_t$, and the Lighthill ξ-shift factors rendering the solution uniformly valid near the new rounded leading-edge.

Further, the device of computing only the (small) perturbation velocities $\Delta\underline{\tilde{u}}_t$, $\Delta\underline{\tilde{u}}_\ell$ from Δe_t, Δe_ℓ, which saves time because the Ledger-Sells routine is adaptive (useful for the first and second problems), breaks down here because

the already-computed velocities are known only on some previously-generated thickness surface, not at the current values of z_t . (An attempt to calculate values on the new thickness surface using Taylor series turned out, not surprisingly, very inaccurate near the leading-edge.) So for this problem it is necessary to work with the complete source and doublet distributions all the time when calculating $\underline{\tilde{u}}_t$ and $\underline{\tilde{u}}_\ell$.

When the program so far described was run, inspection of the results showed that despite the inclusion of Δz_t in the Maclaurin series theory, the successive estimates for Δz_t would be improved if Δz_t was determined only after one Maclaurin series calculation, and not after the Taylor series. Similarly to the second problem, there seems to be a coupling between R_t, Δz_t and the shortfall in Q_u , such that if Δz_t is calculated every time, even though the corresponding linear-theory source distribution is always taken into account, R_t does not converge quickly to zero. By determining Δz_t only half as often, the residual R_t is given more time to settle down; and by determining it after the Maclaurin series calculations, we postpone it as long as possible after the final Ledger-Sells calculation, so that for a given number of these, R_t is likely to be smallest and the last output table of thickness distribution is likely to be nearest to that giving the desired upper-surface pressure distribution.

3.4 Fourth problem: hybrid

In this problem, the upper-surface pressure distribution is again specified everywhere, but different second conditions are imposed inboard and outboard of a spanwise section fairly near the root, $\eta = \eta^*$ say. For $\eta \geqslant \eta^*$ the wing thickness distribution is specified. In the course of iterations on this part of the problem, a doublet distribution $\ell(\xi,\eta)$ is calculated (for $\eta \geqslant \eta^*$) and repeatedly adjusted as in the second problem; it is then necessary to extrapolate ℓ in some way to the inboard region $0 \leqslant \eta < \eta^*$, and one way to do this is simply to require that the computed inboard doublet distribution be independent of spanwise position:

$$\ell(\xi,\eta) = \ell(\xi,\eta^*) \qquad (0 \leqslant \eta < \eta^*) \quad .$$

In linear theory this would be equivalent to maintaining the chordwise load distribution right into the root, and in our problem only small departures from this condition should result. Finally, to satisfy the upper-surface pressure condition for $0 \leqslant \eta < \eta^*$ we adjust the thickness distribution in that region as in the third problem.

The program has been arranged to treat $\eta = \eta^*$ as the third collocation station ourboard from, but not including, the root, so that there are two collocation stations inboard of $\eta = \eta^*$ on which the thickness distribution is to be adjusted. In calculating the thickness perturbations, we consider that it is essential to ensure that the thickness distribution for $\eta \leqslant \eta^*$ always fairs smoothly into the given distribution for $\eta \geqslant \eta^*$, and the most practical way to do this seems, to fit (by least squares) quadratic curves with the required (zero) first derivative spanwise to the calculated thickness perturbations at each value of ξ .

The same curve fit is used to extrapolate the new thickness distribution to the root $\eta = 0$, which is again not a collocation station but is still an output station. This curve fitting means that near the root the upper-surface pressure condition is now satisfied in a mean sense only, at each collocation station value of ξ .

4 RESULTS

4.1 First problem

Results were available for the cambered and twisted RAE Wing 'B'[8] at Mach number 0.8, from the author's direct program[1]. Wing 'B' has planform aspect ratio 6, taper ratio 1/3, straight leading and trailing-edges on each half-wing, and mid-chord sweep angle 30° (Fig.2); the chordwise thickness distribution is that of the 9 per cent thick RAE 101 section. As a test case for the first problem, the final output planar doublet strength from these results was input as data; its behaviour at three spanwise stations, near the root, in mid-semispan and near the tip, is shown in Fig.2a. The program was run for four iterations.

As the planar doublet strength, and hence the velocity field $\underset{\sim}{\tilde{u}}_{\ell}$, is fixed, we may expect the overall spanwise loading properties (which depend only on the doublet distribution in linear theory), the residual error R_{ℓ} and hence the camber and twist distributions, to settle down fairly quickly to their final values; this expectation is borne out by Figs.2b and 2c in which the difference between the spanwise twist and loading distributions calculated at the first and fourth iterations can hardly be seen on the graph. The corresponding camber distributions at three stations are shown in Fig.3, and except near the root, the difference between results for the first and fourth iterations is also very small. Also shown in Figs.2b and 3 are the actual values for Wing 'B', which do exhibit noticeable differences with the converged results. At the outboard

stations in mid-semispan and near the tip, these differences can be attributed to numerical error in the trapezoidal integration method used to evaluate the camber and twist integrals (3-3), (3-4), when data is available only at seven interior Weber points; for this small number of chordwise points, which has been taken for demonstration purposes only, the error in the twist distribution is only of the order 5 per cent, and would be reduced (and more detailed input and output secured) if more chordwise points were taken. The large difference in camber near the root (in Fig.3) is almost certainly due to the absence from the design program of the line singularities introduced at the root in the direct program; although these line singularities have their major effect on the root section, they do have some effect on the calculated planar doublet strength (through cross-coupling with the boundary conditions) at the first outboard station. These factors lead also to a considerable difference between values from direct and design programs in the upper-surface pressure C_{pu} near the root, as shown in Fig.4; however, for the two outboard stations, notwithstanding the slight differences in camber there, the differences between converged values and values from the direct program could hardly be distinguished on this scale, and have been omitted for clarity. Fig.4 shows principally that C_{pu} takes longer (but not unacceptably longer) to settle down than the camber and twist near the root, and slightly longer at the outboard stations; this is because the source distribution has to be adjusted repeatedly to reduce the boundary condition error R_t, and we know from experience with the direct program that this error is likely to be largest near the root, and has a rather uneven convergence ratio.

Results from the program for this first design problem (to which we shall refer as Option 1) have also been used as test cases for the other problems, a procedure which seems likely to produce consistent results as the basic calculation methods, and the principal source of error in these demonstrative cases (in numerical evaluation of the camber and twist integrals), are the same. Also, any comparisons with results from the direct program would be bedevilled by the effects of the line singularities, just as we have already seen for this first problem; by instead taking results from the design program as test data and convergence targets, it is much easier to assess the behaviour of the other design programs near the root.

4.2 Second problem

In the last section we obtained results for RAE Wing 'B' at Mach number 0.8 from the design program Option 1. To gain some experience of the program for the second problem, we input the final upper-surface pressures C_{pu} as a target distribution, along with the original thickness distribution, and again ran the program for four iterations.

The target distributions, and the results from the first and fourth iterations, are shown in Figs.5-7. The targets are the same as the final distributions shown in Figs.2-4, and are now represented by full lines. A first glance at Figs.5b and c for the twist and spanwise loading characteristics suggests that convergence is good at the outboard stations, mid-semispan and near-tip, but that the results are not fully converged near the root; Fig.5a shows that the doublet strength near the root is also converging rather slowly. The camber distributions (Fig.6) tell a similar story: outboard, very good convergence to the target from a rather poor first-iteration result; near the root, still some way to go though the general shape of the curve, including the hump near the root trailing-edge, is well predicted. Fig.7 shows the corresponding behaviour of C_{pu}, and it is rather surprising that the remaining change required in C_{pu} near the root, in particular near the apex, corresponds to so large a remaining change in camber and twist according to Figs.5b and 6. This may be due, amongst other things, to the proximity of the root-line singularity in upwash corresponding to the kinked doublet distribution, so that a small change in doublet strength may produce a large change in upwash, and hence in camber and twist.

It is perhaps worth commenting on the first guess for the doublet strength as shown in Fig.5a. This first guess is calculated using the older version of Lock's method[5] in which the velocity components due to thickness are first estimated using the RAE Standard Method[6]; but it is difficult to see how to improve it substantially, as the accompanying first guess at the source distribution is such that the first estimate for C_{pu} is not too far out near the root, and indeed seems excellent towards the trailing-edge for this case. These results, with the attendant errors in the first estimates of camber and twist shown in Figs.5b and 6, suggest that, in the design problem, second-order effects are very important near the root, and that even though the pressure coefficient C_{pu} from a first-order scheme may be near to the required value, it is necessary to check that the boundary conditions on the wing surface are well satisfied by the velocity fields assumed or implied by such a first-order scheme.

4.3 Third problem

It may happen that a wing can be designed to support a uniform spanwise distribution of upper-surface pressure and of loading near the root, with beneficial aerodynamic consequences, by increasing the section thickness/chord ratio near the root. If this design also avoids an unrealistic increase in root twist, and happens to be structurally sensible and convenient, so much the better.

To provide a test case with a known solution, a wing somewhat similar to RAE Wing 'B' and designated Wing '$\hat{B}$', was designed first, using Option 1. The thickness distribution was specified as the RAE 101 section, the thickness/chord ratio τ being 9 per cent at and outboard of the collocation station $\eta^* = 0.1563$, rising parabolically to 13.5 per cent at the root (see also Fig.8a):

$$\tau = 0.09 \left[1 + 0.5 \left(1 - \frac{\eta}{0.1563} \right)^2 \right] \qquad (\eta \leqslant 0.1563) \ .$$

The behaviour of the specified doublet distribution at three stations, including the inboard region $\eta \leqslant 0.1563$, is shown in Fig.8b. (This choice of doublet distribution was a historical accident based on earlier work on the fourth problem.)

The results from this run, representing the target distributions, are again shown as the continuous lines in the remaining figures. The program was run for five iterations. Fig.8c shows the convergence of the twist distributions, and we see that the target is nearly attained everywhere, and that the first shot was not far wide of the mark either. (In this case, the effect of root thickening on the design root twist is marginal: a degree or so less than the values shown for Wing 'B' in Fig.2b, for the same lift coefficient C_{LL} .)

Fig.9 shows the convergence of the thickness distribution. Considering first the two outboard stations, we see that the results for the third and fifth iterations are virtually identical, and that the corresponding pressure distributions (Fig.10) and camber distributions (Fig.11) are very nearly on target, being indistinguishable except near the leading edge. However, the converged thickness distributions are not quite on target. This must be due to numerical error in integrating $\partial \Delta z_t / \partial \tilde{x}$, like the corresponding numerical error demonstrated for the camber in Fig.3. The relative error seems smaller than that in the camber; a likely mitigating cause is that part of the error in z_t is

picked up when the velocity components are evaluated on the incorrect surface. This error would likewise decrease as the number of collocation points chordwise is increased.

Near the root, the thickness distribution converges very slowly, as the gap between third and fifth iterations in Fig.9 shows. The difference between the results for the fifth iteration and the target distribution is larger than either the remaining convergence leeway we might expect or the numerical error in integration we could anticipate from the results outboard, but can easily be imagined as the sum of these two contributions.

The pressure distribution in this region (Fig.10) also exhibits slow convergence in the first half-chord, but the final shortfall of the target is little different from that outboard. It may be an inherent difficulty for the third problem that the pressure distribution is less sensitive to the thickness distribution near the root than outboard. It is not easy to decide how to cope with this difficulty. An over-relaxation factor of about 2 could be introduced near the root (it is not needed outboard), to speed up the convergence, though we would prefer to build up more experience before citing this as the universal panacea. It would also help if the basic estimate z_{tB} could be improved near the root; inspection of the detailed computer output shows that the improvement obtained with Lock's formula is not remarkable, so that the improvement would need to be fairly drastic; we also note that the basic estimate definitely overpredicts the thickness at the mid-semispan station, whereas the thickness is underpredicted at the root. (There was no zero in the first estimate for z_{tB}, and so this estimate did not have to be modified as described in section 3.3 and Appendix C.) There is also the possibility of setting up an inner iteration cycle for the successive increments Δz_t, as was done for the doublet strength in the second problem, but it is very likely that in this problem the dominant disturbance, not taken into account by the formula (3-7), is the change in the velocity fields of the two singularity distributions when computed on different thickness surfaces, rather than just the change in v_t and w_t due to perturbation sources. These changes could be estimated, using Taylor series, if the program were rearranged to store the field derivatives $\partial \tilde{u}_t/\partial z$, etc. near the root, which are currently overwritten to save core store.

The remaining error in the camber distribution near the root (Fig.11) is obviously associated with the errors in the other field quantities, but is at least an order of magnitude smaller than the remaining error in the thickness

distribution. We might expect this since the camber and twist distributions depend largely on the input doublet strength. On the other hand, the outboard results for the first iteration, which do differ somewhat from the target distributions, show that the agreement in the twist distribution at the same stage (Fig.8c) is probably fortuitous and that second-order effects are important for this problem, outboard as well as near the root.

4.4 Fourth problem

For this final problem, the same test case was chosen as that for the third problem: the wing we have denoted as RAE Wing '$\hat{B}$'. The section separating regions where different conditions are applied was the section where the inboard rise in thickness/chord ratio begins, $\eta = \eta^* = 0.1563$. For this problem, the basic estimate for inboard thickness has not been programmed as in the third problem; instead, the first guess was simply taken to be the same as the fixed outboard distribution, the 9 per cent thick RAE 101 section. The program was again run for five iterations.

The target distributions are again shown as full lines in Figs.12-14. We see that in mid-semispan and near the tip, all quantities converge well, as they did for the second problem, to which this hybrid problem is essentially equivalent outboard. We also observe the same poor nature of the first guess, which corresponds essentially to established first-order techniques, despite the fact that at mid-semispan the chordwise pressure distribution is not too far wrong.

Near the root, as usual, convergence is slow and the thickness distribution (Fig.12a) has not converged to graphical accuracy. But we are somewhat nearer the target than we were in the third problem, and indeed the major part of the remaining error could be just the numerical integration error in Δz_t (Fig.9). Convergence of the root twist (Fig.12b) and camber (Fig.13) is not quite as good as in the third problem, but much better than in the second problem. Here too, improvement on first-order results is noted. The graphs of section lift and centre of pressure duly exhibit the expected spanwise invariance near the root (Fig.12c). The upper-surface pressure distribution has converged to about the same level of accuracy as in the second and third problems (Fig.14); the results near the root have been plotted for the second iteration rather than the first (for which only the *ad hoc* first shot for the thickness distribution was available) to show again the level of error when only one thickness perturbation is calculated.

Wing '$\hat{B}$' is a special case, tailored for this problem so that the root thickness distribution is precisely of the quadratic spanwise form which the inboard least squares fit demands so that no difficulty arises with this smoothing artifice. Moreover, the interaction between the unknown doublet strength and the unknown thickness inboard happens to be favourable, so that overall improvement in convergence is found compared with both the second and third problems. Nevertheless, the results for this hybrid and somewhat pathological problem at least seem promising.

5 CONCLUSION

In this Report we have studied four wing design problems, for two of which the solutions have already been considered in principle by Weber[4]. The implementation of the first problem (given thickness z_t and doublet strength, or first-order loading, ℓ) was straightforward and the program for it (Option 1) converged rapidly.

The second problem (given z_t and the upper-surface pressure distribution C_{pu}) and the third problem (given ℓ and C_{pu}) have been satisfactorily resolved in the outboard wing regions, mid-semispan (more or less sheared-wing station) and, perhaps surprisingly, near the tip; but they have proved far less tractable near the root of a swept wing. For the second problem, the camber and twist are very sensitive to the doublet strength at the root, as we might expect from first-order theory, and there is considerable cross-coupling between ℓ, C_{pu} and the residual error R_t in the symmetric boundary condition. Convergence has been secured for a swept wing at high Mach number, but not for another in incompressible flow, for which it seems likely that the sidewash and upwash velocity components, which are not reduced in scale by the Prandtl-Glauert factor relative to the streamwash, make it almost impossible to find a suitable approximate doublet distribution to satisfy the upper-surface pressure condition near the root trailing edge in the first one or two iterations, so that an optimization technique, yet to be devised, is required. For the third problem, C_{pu} does not seem to be very sensitive to z_t at the root, again R_t has to be allowed to settle down before z_t is adjusted, and convergence is slow. Also, since the velocity fields due to the complete source and doublet distributions have to be computed on each new thickness surface, the program runs for rather longer than Options 1 or 2. But the program (Option 3) has not actually failed to converge for any case for which a solution is known.

The fourth problem is a hybrid of the second and third problems in which ℓ is to be determined outboard, and the thickness distribution inboard of a certain section near the root. In our opinion this hybrid stands an excellent chance of giving the wing designer the solution to his commonest problem outboard, while avoiding the severe practical difficulties encountered near the root in Option 2 and instead determining the required increase of thickness there, to maintain good flow quality and to give additional structural strength. The results for one particular case show better convergence than those from either Options 2 or 3, and while the dangers of arguing from one case are realized, this option (Option 4) seems promising and worth bringing to the attention of designers.

It may be asked why we have used the programs to obtain results for wings at the high subcritical Mach number 0.8, since it is known that the first-order Prandtl-Glauert rule can only be expected to give good results for low subcritical Mach numbers for which the flow nowhere approaches sonic speed. One answer is that a design application can be envisaged at high subcritical Mach numbers, if a shockfree flow is sought and if a shockfree solution of good quality sufficiently close to the design condition is available from another method, or from experiments, which might even be for a wing-body or wing-nacelle combination. In this case, we would assume that changes in wing-body interaction effects due to small perturbations on the given wing are negligible over the major part of the wing. Let us denote the upper-surface pressure distribution from this given solution by $C_{pu,E}$ and that required by $C_{pu,D}$. Using our direct program[1], we can compute the Prandtl-Glauert solution $C_{pu,P}$ for the given isolated wing, and it will exhibit an error $C_{pu,P} - C_{pu,E}$ which would also include the interaction effects in a wing-body combination. Since $C_{pu,D}$ does not differ much from $C_{pu,E}$, we could expect that the wing we seek does not differ much from the datum wing, and that the error in the Prandtl-Glauert solution $\bar{C}_{pu}$ for the wing sought would not differ much from the error in the Prandtl-Glauert solution $C_{pu,P}$ for the datum wing:

$$\bar{C}_{pu} - C_{pu,D} \doteq C_{pu,P} - C_{pu,E}$$

hence

$$\bar{C}_{pu} \doteq C_{pu,D} + C_{pu,P} - C_{pu,E} \ .$$

If, then, we design our wing to have the upper-surface pressure distribution $\bar{C}_{pu}$, it seems likely that the true result will be close to the target distribution $C_{pu,D}$. Which option is used would depend on whether the thickness or the loading distribution is to be retained; we remark that if the thickness distribution is to be retained outboard, Option 4 might be better than Option 2 (since the centre line distributions in the direct program are not reproduced or used in the design programs), but would be less important if the wing thickness can be increased at the root.

It is also worth mentioning briefly a possible use in landing and take-off design studies. The programs cannot be used to design wings with separate slats or other high-lift devices, but they might be used to obtain a suitable camber line for the RAE variable aerofoil mechanism (RAEVAM), which can under some circumstances compete with separate high-lift devices.

Appendix A

LOCK'S FORMULA FOR THE FIRST ESTIMATE OF WING LOAD DISTRIBUTION

Lock[5] has proposed a formula for the total velocity Q on a wing in compressible flow, suitable for use in the design problem:

$$DQ^2 = \left[\cos\alpha + \frac{\beta_n}{B_n}\left\{u_{tB}\cos\alpha \pm u_{\ell B}\left(1 + \frac{S^{(3)}}{B_n}\sec\Lambda_m^*\right)\right\}\right]^2 + \frac{\beta_n^2}{B_n^2}\left[v_{tB}\cos\alpha \pm v_{\ell B}\left(1 + \frac{S^{(3)}}{B_n}\sec\Lambda_m^*\right)\right]^2 + \left(1 - \kappa_2^2\right)(D - 1)\sin^2\Lambda_x\cos^2\alpha \qquad (A\text{-}1)$$

where the upper signs are taken on the upper surface;

α is the local section incidence, and is therefore equal to our α_T ;

Λ_x is the local sweep angle on physical wing;

Λ_m is sweep angle of maximum thickness line on physical wing;

$\begin{pmatrix}\Lambda_x^*\\ \Lambda_m^*\end{pmatrix} = (1 - |\kappa_2|)\begin{pmatrix}\Lambda_x\\ \Lambda_m\end{pmatrix}$;

κ_2 is a spanwise interpolation function, taken as in section 5.2 of Ref.1;

$\beta_n = \left(1 - M_\infty^2\cos^2\Lambda_x\right)^{\frac{1}{2}}$;

$B_n = \left\{\beta_n^2 + M_\infty^3\cos\Lambda_x\left(1 - |\kappa_2|\sin^2\Lambda_x\right)"C_{pi}"\right\}^{\frac{1}{2}}$; it is suggested[5] that $"C_{pi}"$ should be obtained by writing $B_n = 1$ in (A-1), giving $Q = "Q_i"$, and taking $"C_{pi}" = 1 - "Q_i"^2$;

$D = 1 + \sec^2\Lambda_x^*\left(\frac{\partial z_w}{\partial x}\right)^2\Big/\beta_n^2$;

$u_{tB}(x,y,0)$, $v_{tB}(x,y,0)$ are estimates from linear theory for the velocity components due to wing thickness, for example, see Ref.1;

$u_{\ell B}(x,y,0)$, $v_{\ell B}(x,y,0)$ represent the thin-wing components due to doublets in linear theory, and are to be determined;

$S^{(3)}$ represents the second-order interaction effect between wing thickness and incidence.

It is convenient to mention two details here. First, Lock's formula is a semi-empirical extension of the Goethert rule to take into account higher-order compressibility corrections through the factor B_n. Since our method is based on the affine transformation which yields the Goethert rule, there is no point in including these higher-order terms $O(M_\infty^3)$ in B_n, and so we simply take $B_n = \beta_n$. This reduces (A-1) to equation (3-5) of the main text.

Secondly, we have slightly modified the classical derivation of $S^{(3)}$ to derive an expression which seems more consistent with the problem at hand than the one given in Ref.6, even though it is only one of the several second-order effects present, and only holds for two-dimensional swept wings. Consider such a wing, with uniform sweep angle $\Lambda_x = \Lambda$, and incidence α. The analogous wing will have the uniform sweep angle $\tilde{\Lambda}$ where

$$\tan \Lambda = \beta \tan \tilde{\Lambda} \quad .$$

We have, for the thin-wing velocity components,

$$v_{\ell B} = - u_{\ell B} \tan \Lambda \tag{A-2}$$

and hence, with $u_{\ell B} = \tilde{u}_{\ell B}/\beta$, we have the corresponding relation for the analogous wing in affine space:

$$v_{\ell B} = - \tilde{u}_{\ell B} \tan \tilde{\Lambda} \quad .$$

The first-order boundary condition $w_{\ell B} = - \alpha$ is satisfied by the doublet distribution ℓ_B with

$$\tilde{u}_{\ell B} = \tfrac{1}{4} \ell_B = \alpha \left(\frac{1 - \xi}{\xi} \right)^{\frac{1}{2}} \cos \tilde{\Lambda} \quad .$$

The second-order boundary condition gives:

$$\Delta w_\ell = \frac{\tilde{u}_{\ell B}}{\beta^2} \frac{\partial z_t}{\partial \tilde{x}} + v_{\ell B} \frac{\partial z_t}{\partial y} - z_t \frac{\partial w_{\ell B}}{\partial z} \quad .$$

Using the sheared-wing relation $\partial/\partial y = - \tan \tilde{\Lambda} \, \partial/\partial \tilde{x}$, and the zero divergence of $\underline{\tilde{u}}_{\ell B}$ in our affine space, we obtain

$$\Delta w_\ell = \left(\frac{1}{\beta^2} + \tan^2\tilde{\Lambda}\right)\tilde{u}_{\ell B}\frac{\partial z_t}{\partial \tilde{x}} + z_t\frac{\partial \tilde{u}_{\ell B}}{\partial \tilde{x}}\left(1 + \tan^2\tilde{\Lambda}\right)$$

$$= \alpha\left(\frac{1-\xi}{\xi}\right)^{\frac{1}{2}}\cos\tilde{\Lambda}\sec^2\tilde{\Lambda}\left[\left(\frac{\cos^2\tilde{\Lambda}}{\beta^2} + \sin^2\tilde{\Lambda}\right)\frac{\partial z_t}{\partial \tilde{x}} - \frac{z_t}{\tilde{c}}\frac{1}{2\xi(1-\xi)}\right] .$$

$\tilde{c}$ is the analogous wing chord. Transforming the square bracket to physical variables, and noting that

$$\frac{\cos\tilde{\Lambda}}{\beta} = \frac{\cos\Lambda}{\beta_n} \quad ; \qquad \sin\tilde{\Lambda} = \frac{\sin\tilde{\Lambda}}{\beta_n} \tag{A-3}$$

we get

$$\Delta w_\ell = \alpha\left(\frac{1-\xi}{\xi}\right)^{\frac{1}{2}}\frac{\beta}{\cos\tilde{\Lambda}}\left[\frac{\partial z_t/\partial x}{\beta_n^2} - \frac{z_t/c}{2\xi(1-\xi)}\right] .$$

We satisfy this boundary condition by a doublet strength $\Delta\ell$ giving the further streamwash

$$\Delta\tilde{u}_\ell = \tfrac{1}{4}\Delta\ell = \frac{1}{\pi}\left(\frac{1-\xi}{\xi}\right)^{\frac{1}{2}}\cos\tilde{\Lambda}\int_0^1 \Delta w_\ell(\xi')\left(\frac{\xi'}{1-\xi'}\right)^{\frac{1}{2}}\frac{d\xi'}{\xi - \xi'}$$

$$= \tilde{u}_{\ell B}\frac{\beta}{\cos\tilde{\Lambda}}\frac{1}{\beta_n^2}S^{(3*)}$$

where $S^{(3*)} = \frac{1}{\pi}\int_0^1\left[\frac{\partial z_t}{\partial x} - \frac{z_t}{c}\frac{\beta_n^2}{2\xi'(1-\xi')}\right]\frac{d\xi'}{\xi - \xi'}$.

This integral differs from the standard definition of $S^{(3)}$ by the presence of β_n^2 in the integrand.

Using (A-3) again, we have finally

$$u_\ell = u_{\ell B} + \Delta u_\ell = u_{\ell B}\left[1 + \frac{\sec\Lambda}{\beta_n}S^{(3*)}\right] ,$$

and similarly for v_ℓ ; and these are the formulae customarily modified to give (A-1).

To obtain a first estimate for $u_{\ell B}$, Lock[5] now replaces $\cos \alpha_T$ by 1, while α_T is still an unknown quantity, and z_w by z_t in the expression for D ; and the dependence of $v_{\ell B}$ on $u_{\ell B}$ is taken to be similar to that exhibited for the sheared wing by (A-2):

$$v_{\ell B} \simeq - u_{\ell B} \tan \Lambda_v \qquad \text{(A-4)}$$

where $\tan \Lambda_v = \left[\beta_n^2 \dfrac{\cos^2(\lambda \tilde{\Lambda}_m)}{\cos^2 \Lambda_m} - \beta^2\right]^{\frac{1}{2}} = \beta\left[\dfrac{\cos^2(\lambda \tilde{\Lambda}_m)}{\cos^2 \tilde{\Lambda}_m} - 1\right]^{\frac{1}{2}}$.

Finally, Q is put equal to the design value $\bar{Q}$. Then (A-1) becomes a quadratic in the variable $X = u_{\ell B}\left[1 + S^{(3)} \sec \Lambda_m^*/\beta_n\right]$:

$$AX^2 + 2BX + C = 0$$

where $A = \sec^2 \Lambda_v$

$$B = 1 + u_{tB} - v_{tB} \tan \Lambda_v$$

$$C = (1 + u_{tB})^2 + v_{tB}^2 + \left(1 - \kappa_2^2\right)(D - 1) \sin^2 \Lambda_x - D\bar{Q}^2 .$$

Since B is of the order (1 + small quantities), the required solution is

$$X = \left[(B^2 - AC)^{\frac{1}{2}} - B\right]/A .$$

Hence follow the estimates for $u_{\ell B}$ and the affine doublet strength:

$$\ell_B = 4\tilde{u}_{\ell B} = 4\beta u_{\ell B} .$$

Since a small change in $v_{\ell B}$ has a second-order effect on the value of (A-1) compared with that of a small change in $u_{\ell B}$, we can discard the assumption (A-4) and replace $v_{\ell B}$ in (A-1) by the value calculated from the first estimate $u_{\ell B}$ and the more accurate formula[1]:

$$v_{\ell B} = \frac{\partial}{\partial \bar{\eta}}\left[\tilde{c}(\eta) \int_0^{\xi} \tilde{u}_{\ell}(\xi';\eta) d\xi'\right] - \tilde{u}_{\ell B} \tan \tilde{\Lambda} .$$

From ℓ_B we can also compute the first estimate α_{TB} for the twist and write $\cos \alpha = \cos \alpha_{TB}$ in (A-1). This leads to a revised estimate $u'_{\ell B}$ given by

$$u'_{\ell B} = \frac{X'}{1 + S^{(3)} \sec \Lambda^*_m/\beta_n}$$

where $X' = - (1 + u_{tB}) \cos \alpha_{TB}$

$$+ \left[D\bar{Q}^2 - \left\{ v_{tB} \cos \alpha_{TB} + v_{\ell B}\left(1 + S^{(3)} \sec \Lambda^*_m/\beta_n\right)\right\}^2 \right.$$

$$\left. - \left(1 - \kappa_2^2\right)(D - 1) \sin^2\Lambda_x \cos^2\alpha_{TB} \right]^{\frac{1}{2}} .$$

Lock's formula can also be used to modify an initial crude guess for the thickness distribution z_t in the third problem, when the doublet strength is known. From the doublet strength, we can find $u_{\ell B}$ and $v_{\ell B}$. We now assume that u_{tB} in the second term dominates equation (A-1), just as we assumed that $u_{\ell B}$ in the same term dominated the equation when the doublet strength was unknown; we find v_{tB}, D and $S^{(3)}$ from the initial guess for the z_t distribution, and then a revised estimate u'_{tB} is given by

$$u'_{tB} = \left\{ \left[D\bar{Q}^2 - \left\{ v_{tB} \cos \alpha_{TB} + v_{\ell B}\left(1 + S^{(3)} \sec \Lambda^*_m/\beta_n\right)\right\}^2 \right.\right.$$

$$\left. - \left(1 - \kappa_2^2\right)(D - 1) \sin^2\Lambda_x \cos^2\alpha_{TB} \right]^{\frac{1}{2}}$$

$$\left. - u_{\ell B}\left(1 + S^{(3)} \sec \Lambda^*_m/\beta_n\right) - \cos \alpha_{TB} \right\} \Big/ \cos \alpha_{TB} .$$

Appendix B

MODIFICATION OF PERTURBATION QUANTITIES WITH MACLAURIN SERIES

The main iteration cycle involves the execution of the lengthy Ledger-Sells subroutine to obtain the velocity fields $\Delta\underline{\tilde{u}}_t$, $\Delta\underline{\tilde{u}}_\ell$ (or $\underline{\tilde{u}}_t$, $\underline{\tilde{u}}_\ell$) accurately. We might obtain a considerable saving in computing time if we could in effect perform one iteration cycle by using suitable estimates for these velocity fields instead; we would then hope that any errors due to the estimates would be small enough to be absorbed in the main iteration cycle the next time the velocity fields are accurately calculated.

For convenience, we drop the bracketed iteration superscripts from all quantities except the residual errors $R(= \pm R_t + R_\ell)$. Let us suppose that in the nth iteration cycle we have computed $\underline{\tilde{u}} = \underline{\tilde{u}}_t + \underline{\tilde{u}}_\ell$ and the camber and twist distributions z_s, α_T, and have determined perturbation source (and possibly doublet) distributions Δq, $\Delta\ell$ and perturbation camber and twist distributions Δz_s, $\Delta\alpha_T$ to cancel the residual field

$$R^{(n)} = \left(1 + \frac{\tilde{u}}{\beta}\right)\frac{1}{\beta}\frac{\partial z_w}{\partial \tilde{x}} + v\frac{\partial z_w}{\partial y} - \alpha_T - w$$

on the wing surface $z = z_w$.

The next residual field on the perturbed surface $z = z_w + \Delta z_w$ will be (suppressing the x,y-dependence)

$$\begin{aligned} R^{(n,1)} = {} & \left[1 + \frac{\tilde{u}(z_w + \Delta z_w)}{\beta} + \frac{\Delta\tilde{u}(z_w + \Delta z_w)}{\beta}\right]\frac{1}{\beta}\left(\frac{\partial z_w}{\partial \tilde{x}} + \frac{\partial \Delta z_w}{\partial \tilde{x}}\right) \\ & + \left[v(z_w + \Delta z_w) + \Delta v(z_w + \Delta z_w)\right]\left(\frac{\partial z_w}{\partial y} + \frac{\partial \Delta z_w}{\partial y}\right) \\ & - (\alpha_T + \Delta\alpha_T) - \left[w(z_w + \Delta z_w) + \Delta w(z_w + \Delta z_w)\right] . \end{aligned}$$

In this expression, $\underline{\tilde{u}}$, z_w and α_T are first-order small quantities while $\Delta\underline{\tilde{u}}$, Δz_w and $\Delta\alpha_T$ are (at least) second-order small quantities, being derived from such expressions as $R^{(n)}$ which is itself second-order. We therefore expand $R^{(n,1)}$ in powers of Δz_w and retain only quantities up to and including third-order, ignoring for instance terms $O(\tilde{u}z_w\Delta z_w)$, $O(\Delta\tilde{u}\Delta z_w)$. With all quantities again evaluated at $z = z_w$, this leads to

$$R^{(n,1)} = R^{(n)} - \Delta w + \frac{1}{\beta}\frac{\partial \Delta z_w}{\partial \tilde{x}} - \Delta\alpha_T$$

$$+ \frac{\tilde{u}}{\beta^2}\frac{\partial \Delta z_w}{\partial \tilde{x}} + \frac{\Delta\tilde{u}}{\beta^2}\frac{\partial z_w}{\partial \tilde{x}} + v\frac{\partial \Delta z_w}{\partial y} + \Delta v\frac{\partial z_w}{\partial y} - \Delta z_w\frac{\partial w}{\partial z} \quad .$$

We now further expand $\underline{\tilde{u}}$ in powers of z_w (Maclaurin series), so that from this point on all quantities are evaluated at $z = 0$, and continue to retain terms up to third order. We can ignore further contributions from the second line which is already third-order. Thus only Δw contributes further to the expansion:

$$\Delta w(z_w) = \Delta w(0) + z_w\frac{\partial \Delta w}{\partial z} + 0\left(z_w^2 \Delta w\right) \quad .$$

We have already taken our perturbation source, camber and twist distributions according to equations (3-1), (3-2) to make

$$R^{(n)} - \Delta w(0) + \frac{1}{\beta}\frac{\partial \Delta z_w}{\partial \tilde{x}} - \Delta\alpha_T = 0 \quad .$$

We also have

$$-\frac{\partial w}{\partial z} = \frac{\partial \tilde{u}}{\partial \tilde{x}} + \frac{\partial v}{\partial y}$$

and a similar relation for Δw. Hence we can eliminate w, Δw and obtain

$$R^{(n,1)} = \left(\frac{1}{\beta^2} - 1\right)\left[\tilde{u}\frac{\partial \Delta z_w}{\partial \tilde{x}} + \Delta\tilde{u}\frac{\partial z_w}{\partial x}\right] + \frac{\partial}{\partial \tilde{x}}\left(z_w\Delta\tilde{u} + \tilde{u}\Delta z_w\right) + \frac{\partial}{\partial y}\left(z_w\Delta v + v\Delta z_w\right) \quad .$$

Proceeding on the lines of section 2, we write for upper and lower wing surfaces

$$z_w = \pm z_t + z_s \quad ; \qquad \Delta z_w = \pm \Delta z_t + \Delta z_s$$

and

$$\tilde{u} = \tilde{u}_t \pm \tilde{u}_\ell$$

with similar expressions for v, $\Delta\tilde{u}$, Δv. (For the first and second design problems, $\Delta z_t = 0$; and for the first and third problems, $\Delta\tilde{u}_\ell = \Delta v_\ell = 0$.) $R^{(n,1)}$ now splits into $\pm R_t^{(n,1)} + R_\ell^{(n,1)}$ with

$$R_t^{(n,1)} = \left(\frac{1}{\beta^2} - 1\right)\left[\Delta\tilde{u}_t \frac{\partial z_t}{\partial \tilde{x}} + \Delta\tilde{u}_\ell \frac{\partial z_s}{\partial \tilde{x}} + \tilde{u}_t \frac{\partial \Delta z_t}{\partial \tilde{x}} + \tilde{u}_\ell \frac{\partial \Delta z_s}{\partial \tilde{x}}\right]$$

$$+ \frac{\partial}{\partial \tilde{x}}\left(z_t \Delta\tilde{u}_t + z_s \Delta\tilde{u}_\ell + \tilde{u}_t \Delta z_t + \tilde{u}_\ell \Delta z_s\right)$$

$$+ \frac{\partial}{\partial y}\left(z_t \Delta v_t + z_s \Delta v_\ell + v_t \Delta z_t + v_\ell \Delta z_s\right)$$

$$R_\ell^{(n,1)} = \left(\frac{1}{\beta^2} - 1\right)\left[\Delta\tilde{u}_t \frac{\partial z_s}{\partial \tilde{x}} + \Delta\tilde{u}_\ell \frac{\partial z_t}{\partial x} + \tilde{u}_t \frac{\partial \Delta z_s}{\partial \tilde{x}} + \tilde{u}_\ell \frac{\partial \Delta z_t}{\partial \tilde{x}}\right]$$

$$+ \frac{\partial}{\partial \tilde{x}}\left(z_t \Delta\tilde{u}_\ell + z_s \Delta\tilde{u}_t + \tilde{u}_t \Delta z_s + \tilde{u}_\ell \Delta z_t\right)$$

$$+ \frac{\partial}{\partial y}\left(z_t \Delta v_\ell + z_s \Delta v_t + v_t \Delta z_s + v_\ell \Delta z_t\right) \quad .$$

When $\Delta z_w = 0$, these expressions reduce to those given in Ref.1. As in that document, we must ensure that they are uniformly valid near the wing leading edge $\xi = 0$. We require at worst

$$R_t = O(\xi^{-\frac{1}{2}}) \quad ; \qquad R_\ell = O(1) \quad .$$

These expressions are satisfactory except for the second and fourth terms in the square brackets in $R_\ell^{(n,1)}$. We introduce a Riegels type factor and replace this square bracket ($R^*_{c\ell}$, say) by

$$R_{c\ell} = \Delta\tilde{u}_t \frac{\partial z_s}{\partial \tilde{x}} + \tilde{u}_t \frac{\partial \Delta z_s}{\partial \tilde{x}} + \hat{R}_\ell \Big/ \left(1 + \hat{R}_\ell^2\right)$$

with

$$\hat{R}_\ell = \Delta\tilde{u}_\ell \frac{\partial z_t}{\partial \tilde{x}} + \tilde{u}_\ell \frac{\partial \Delta z_t}{\partial \tilde{x}} \quad .$$

This completes the derivation of residual errors by Maclaurin series.

To estimate these residuals, given Δq and perhaps $\Delta\ell$, we need quick estimates for four velocity components on the chordal plane $z = 0$. We use the approximations for $\Delta\tilde{u}_t$, Δv_t (derived from the Standard Method[6]) and $\Delta\tilde{u}_\ell$, Δv_ℓ as set out in equations (5-12) to (5-17) of Ref.1. We also need $\tilde{u}_t$, etc. which

are just the accumulated $\Delta\tilde{u}_t$, etc. on the plane $z = 0$. However, instead of simply accumulating them, after each main iteration we reset $\tilde{u}_t$ by a Taylor series based on the accurate value at $z = z_t$;

$$\tilde{u}_t(0) \doteq \tilde{u}_t(z_t) - z_t \frac{\partial \tilde{u}_t}{\partial z}$$

and similarly for v_t, $\tilde{u}_\ell$, v_ℓ . This avoids the possibility of large errors piling up in the accumulated estimates for $\tilde{u}_t$, etc.

Appendix C

AN IMPROVISED FIRST ESTIMATE FOR WING THICKNESS NEAR THE TRAILING EDGE

When solving the third design problem, if the first estimate for the wing thickness takes negative values near the trailing edge on any section, we improvise a distribution to replace the first estimate in that region temporarily, until the main iteration scheme gets under way. In such a plane section η = constant , let us denote the first chordwise collocation point downstream of the estimated maximum thickness position by $\hat{\xi}$, and denote the estimated thickness by $\hat{z}$ and its derivative by $\hat{v}$ at $\xi = \hat{\xi}$. Then we would like to have a curve $G(\xi)$ which passes through $(\hat{\xi},\hat{z})$ and has the same derivative $G'(\hat{\xi}) = \hat{v}$, becomes rapidly linear further downstream and vanishes at the trailing edge $\xi = 1$. A function which becomes rapidly linear for $\xi > \hat{\xi}$ and contains three unknowns, a, b, c with which to satisfy the other three conditions is

$$G = ae^{-k(\xi-\hat{\xi})} + b\xi + c \qquad (\hat{\xi} \leqslant \xi \leqslant 1)$$

where we arbitrarily choose k so that

$$\lambda \equiv k(1 - \hat{\xi}) = 2$$

so that the exponential term dies out near $\xi = 1$. λ is an adjustable program constant. The other three conditions, in order, now give:

$$\begin{aligned} a + b\hat{\xi} + c &= \hat{z} \\ -ka + b &= \hat{v} \\ ae^{-\lambda} + b + c &= 0 \ . \end{aligned}$$

The solution of these equations is written:

$$a = \frac{\hat{v}(1 - \hat{\xi}) + \hat{z}}{1 - e^{-\lambda} - \lambda}$$

$$b = ka + \hat{v}$$

$$c = \hat{z} - a - b\hat{\xi} \ .$$

We observe, as a check, that a vanishes and G becomes precisely linear if

$$\hat{v} = -\hat{z}/(1 - \hat{\xi})$$

which is the slope of the straight line joining the two end points $(\hat{\xi},\hat{z})$ and $(1,0)$.

SYMBOLS

c	local chord
C_p	pressure coefficient
e_ℓ	doublet function $\ell \sin \phi$
ℓ	planar doublet strength (loading)
M_∞	free stream Mach number
q	planar source strength
Q	local speed
R_t	residual error in symmetric boundary condition
R_ℓ	residual error in antisymmetric boundary condition
s	semispan (taken as 1)
$\underline{u}$	general perturbation velocity vector
$\underline{\tilde{u}}$	general perturbation velocity in affine space
u, v, w	components of $\underline{u}$
$\underline{U}_\infty$	free stream velocity vector
$\underline{U}$	complete velocity vector: $\underline{U}_\infty + \underline{u}_t + \underline{u}_\ell$
U, V, W	components of $\underline{U}$
x, y, z	local Cartesian coordinates for section
x_L	leading-edge ordinate
z_t	wing thickness ordinate
z_s	wing camber ordinate
z_w	wing section ordinate: $z_s \pm z_t$
α_T	local section twist
α	wing incidence (taken as 0)
β	Prandtl-Glauert factor: $\sqrt{1 - M_\infty^2}$
η	y/s
$\bar{\eta}$	y ; but $\partial/\partial\bar{\eta}$ denotes differentiation along lines of constant ξ
η^*	$\eta = \eta^*$ is section dividing root and outboard regions in fourth (hybrid) problem
$\tilde{\Lambda}$	local sweep in affine space (i.e. on analogous wing)
ξ	section percentage-chord: $x = x_L(y) + c(y)\xi$
σ	$\frac{1}{\pi}\int_0^1 \left(\frac{\partial \Delta z_t}{\partial \tilde{x}}\right)_{\xi'} \frac{d\xi'}{\xi - \xi'}$
ϕ	angular chordwise coordinate: $\xi = \frac{1}{2}(1 - \cos \phi)$
Ω_v	under-relaxation factor applied to estimate of output by vortex lattice technique

SYMBOLS (concluded)

Suffices

B	basic estimate
ℓ	due to doublets
t	due to sources
u	value on upper surface

Oversymbols

-	design quantities (e.g. $\bar{C}_{pu}$, $\bar{Q}_u$)
~	quantities in affine space (e.g. $\tilde{x} = x/\beta$, $\tilde{u} = u\beta$)

REFERENCES

No.	Author	Title, etc.
1	C.C.L. Sells	Iterative method for thick cambered wings in subcritical flow. ARC R & M 3786 (1974)
2	J.A. Ledger	Computation of the velocity field induced by a planar source distribution, approximating a symmetrical non-lifting wing in subsonic flow. ARC R & M 3751 (1972)
3	C.C.L. Sells	Calculation of the induced velocity field on and off the wing plane for a swept wing with given load distribution. ARC R & M 3725 (1970)
4	J. Weber	Second-order small-perturbation theory for finite wings in incompressible flow. ARC R & M 3759 (1972)
5	R.C. Lock	Revised compressibility corrections in subsonic swept wing theory, with applications to wing design. NPL Aero. Memorandum 64 (1969)
6	-	Method for predicting the pressure distribution on swept wings with subsonic attached flow. R. Aero. Soc. Transonic Data Memorandum 6312 (1963); Revised version, Eng. Sci. Data Unit Item 73012 (1973)
7	J. Weber	The calculation of the pressure distribution on the surface of thick cambered wings and the design of wings with given pressure distribution. ARC R & M 3026 (1955)
8	A.F. Jones P.V. Grey-Wilson	The design and definition of a particular three-dimensional swept wing. MOD(PE) unpublished work
9	A. Roberts K. Rundle	The computation of first-order compressible flow about wing-body configurations. Report Aero MA 20, BAC, Weybridge (1973)

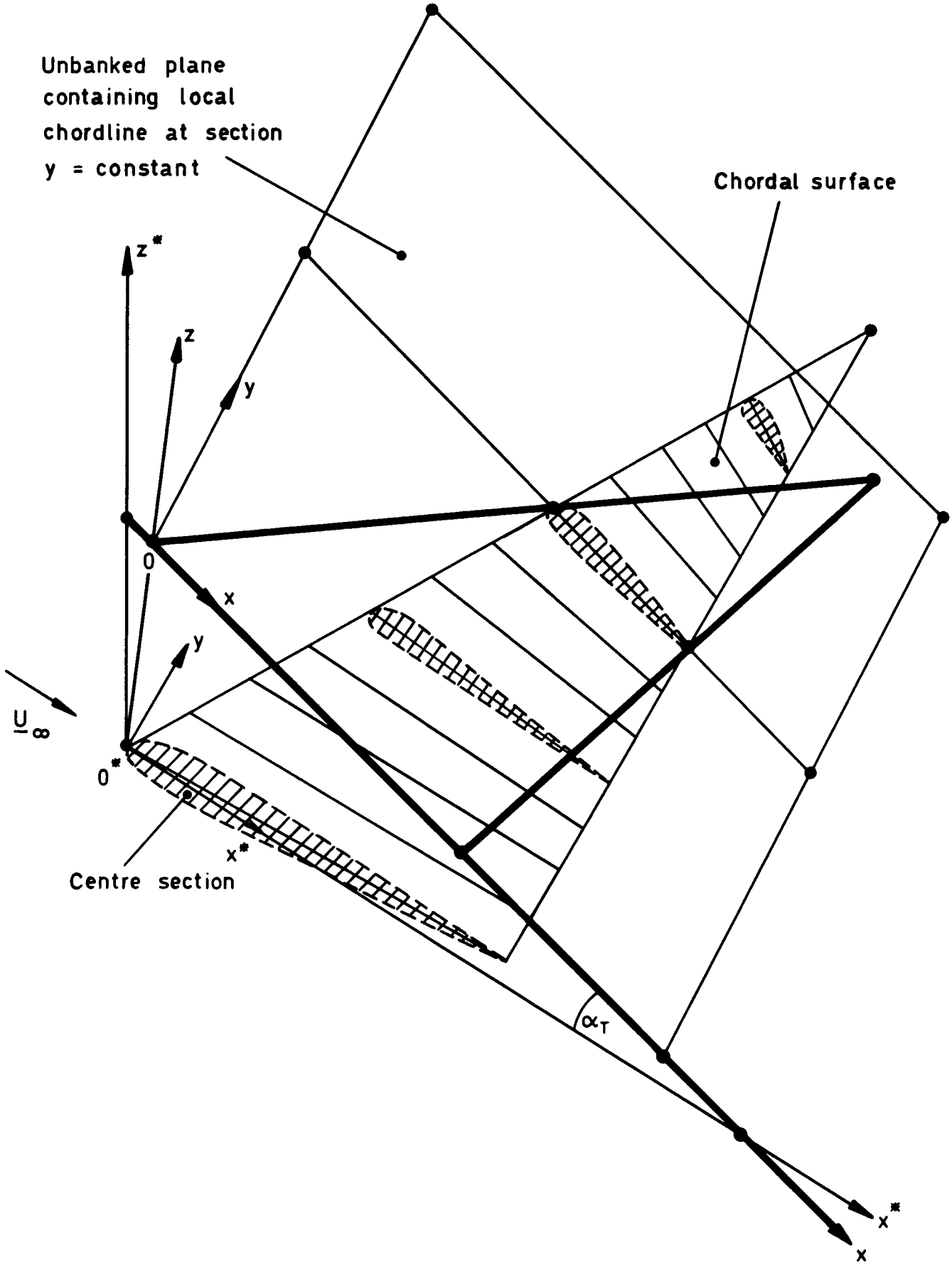

Fig. 1 Sketch of half wing and typical singularity plane

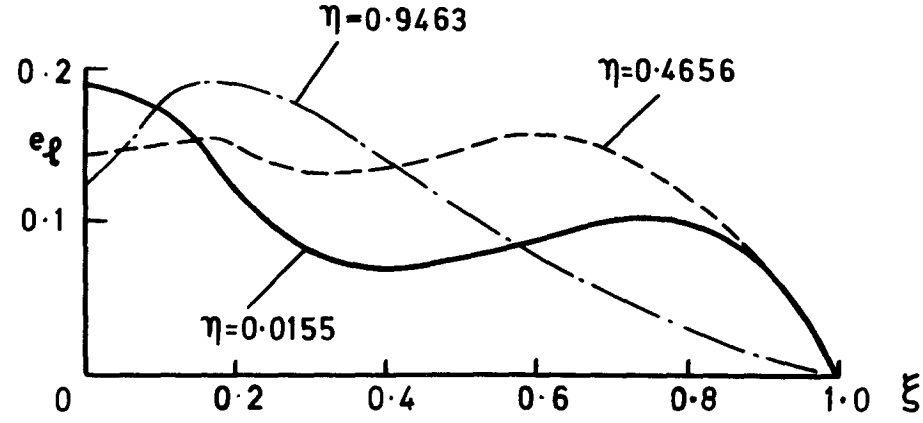

a Design doublet (first-order chordwise load) function

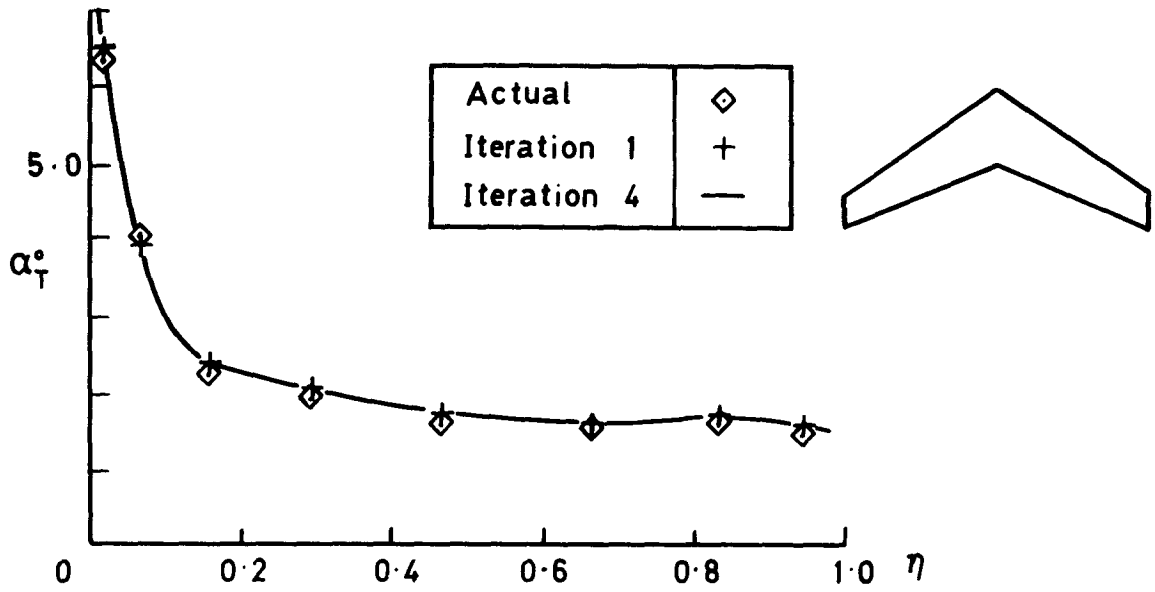

b Iterates for twist distribution

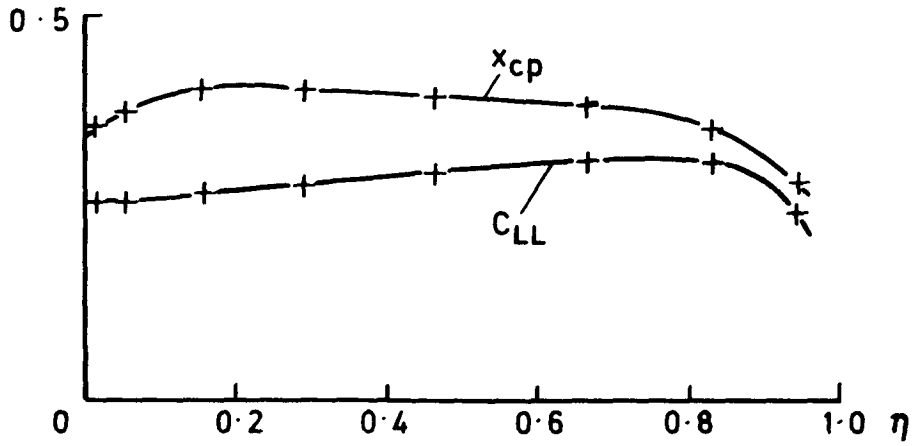

c Iterates for section lift and centre of pressure

Fig.2a-c Details for RAE wing "B", M_∞ =0·8. Problem 1

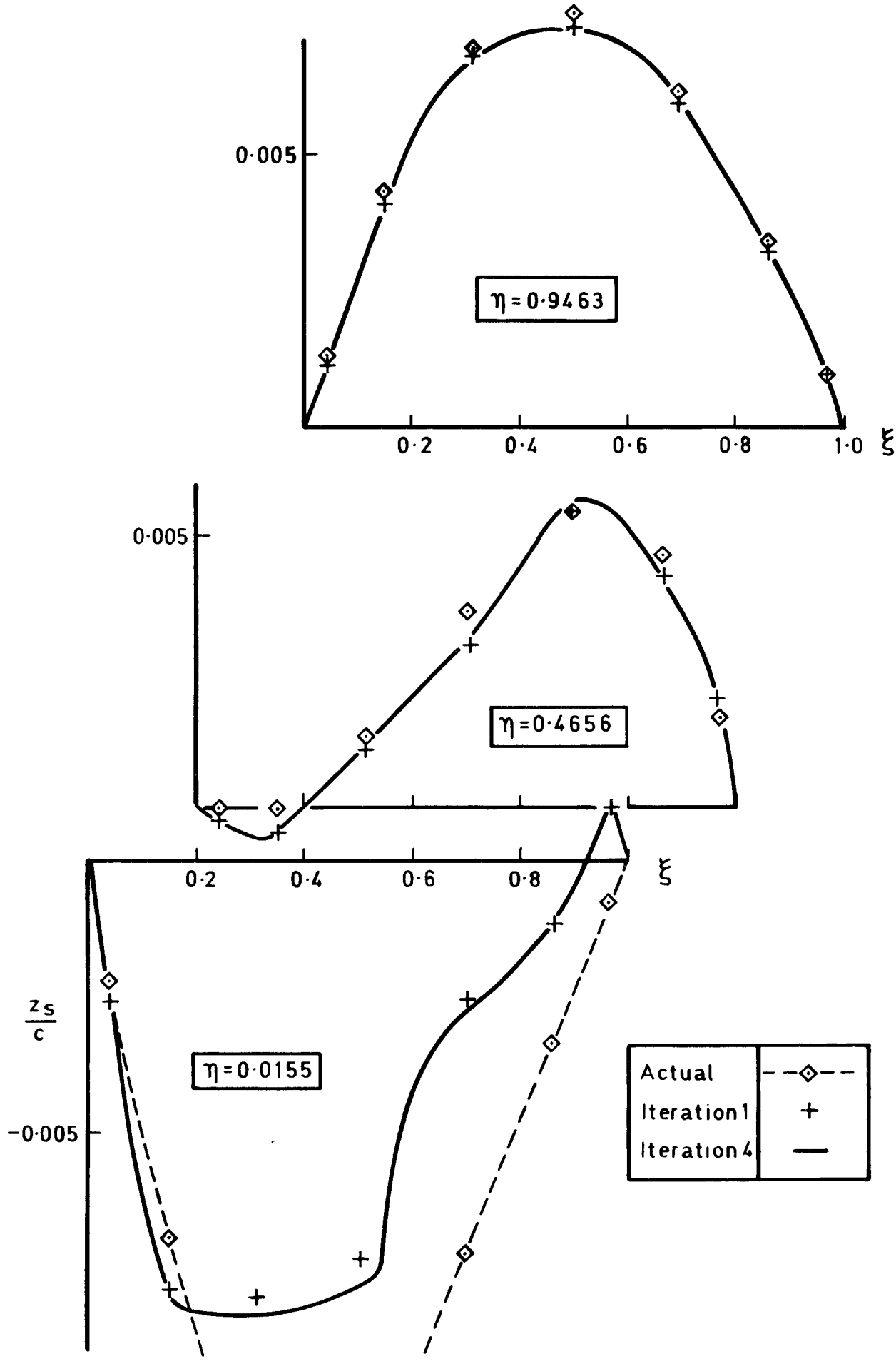

Fig.3 Iterates for camber distribution on RAE wing "B", $M_\infty = 0 \cdot 8$. Problem 1

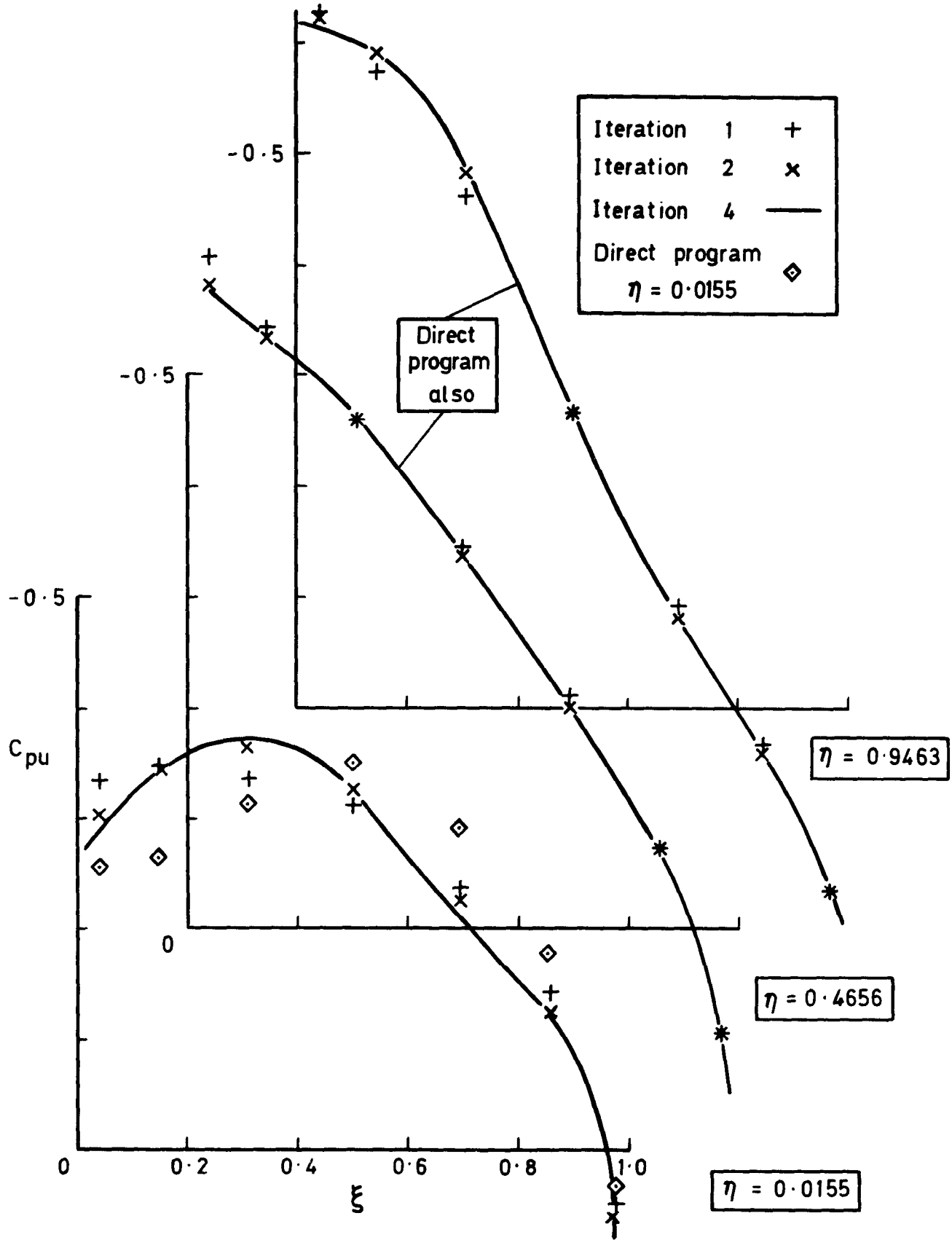

Fig. 4 Iterates for upper-surface pressure distribution on RAE wing "B", $M_\infty = 0 \cdot 8$. Problem 1

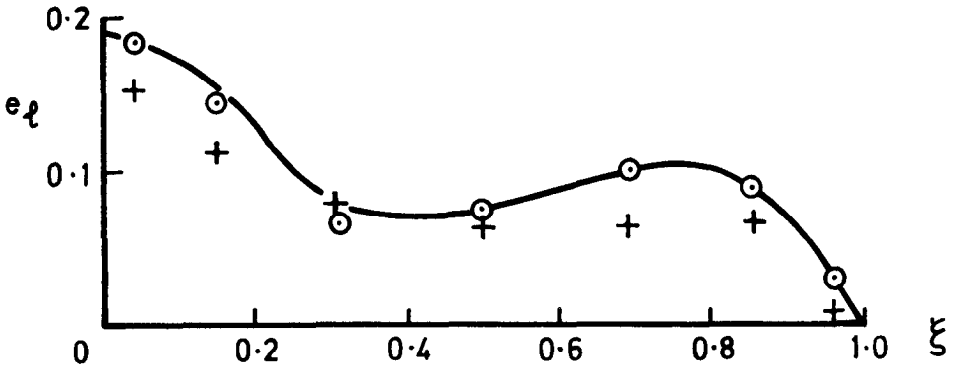

a Doublet function near root (η=0·0155)

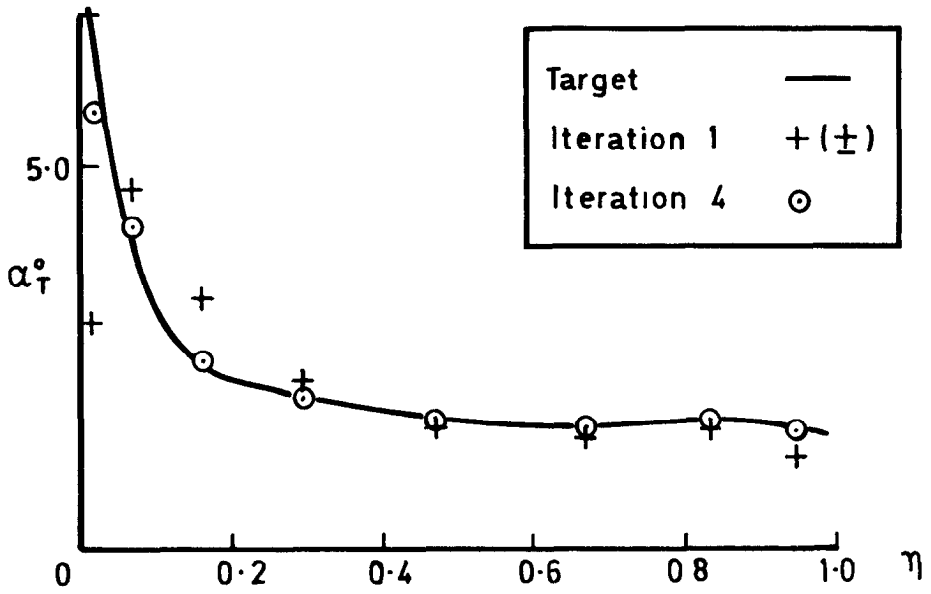

b Twist distribution

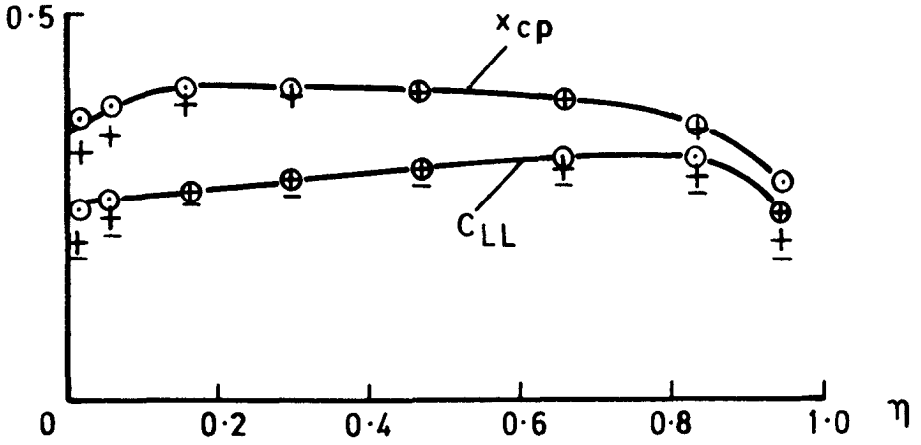

c Section lift and centre of pressure

Fig.5a-c Iterates for RAE wing "B", M_∞=0·8. Problem 2

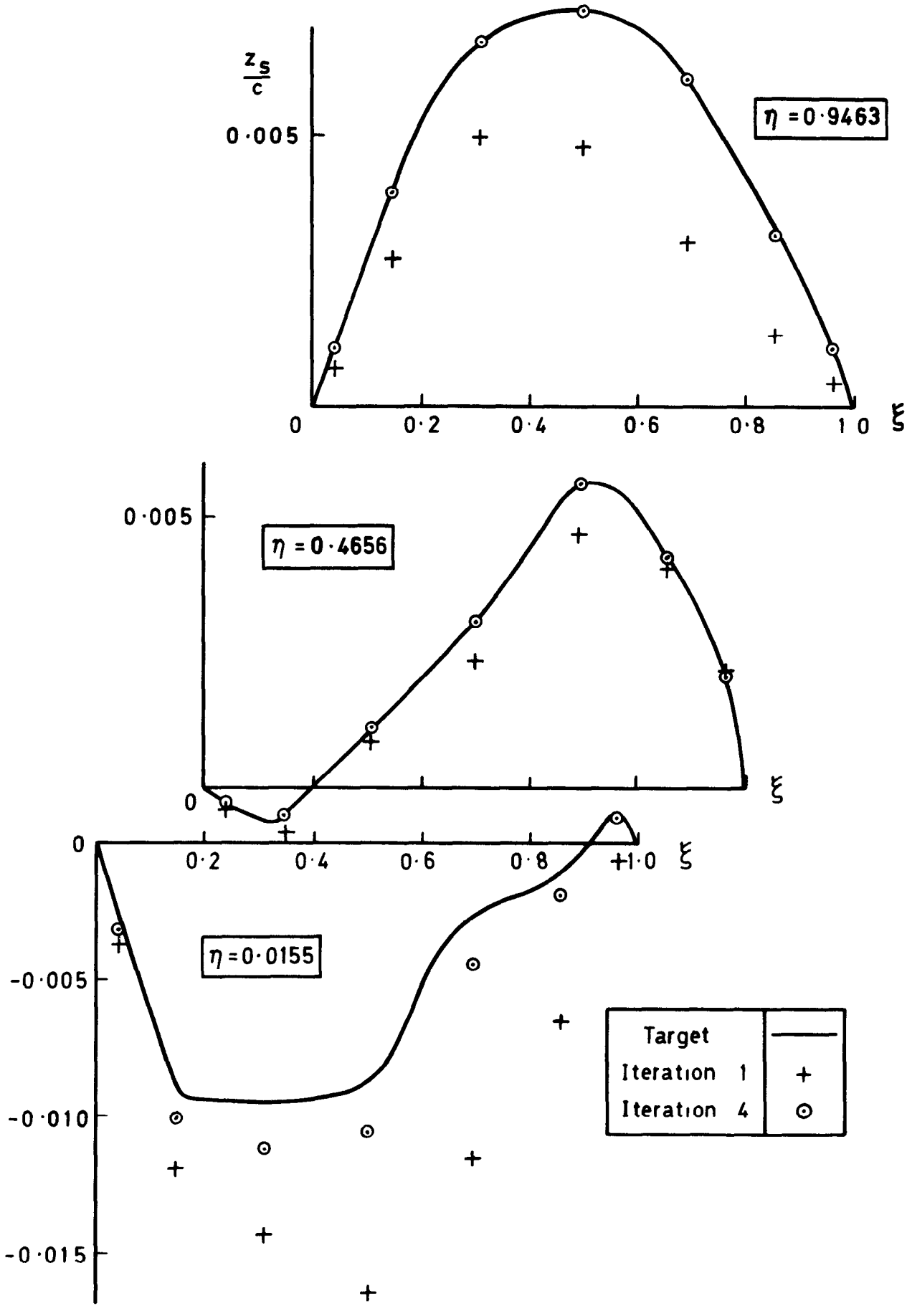

Fig. 6 Iterates for camber distribution on RAE wing "B", $M_\infty = 0 \cdot 8$. Problem 2

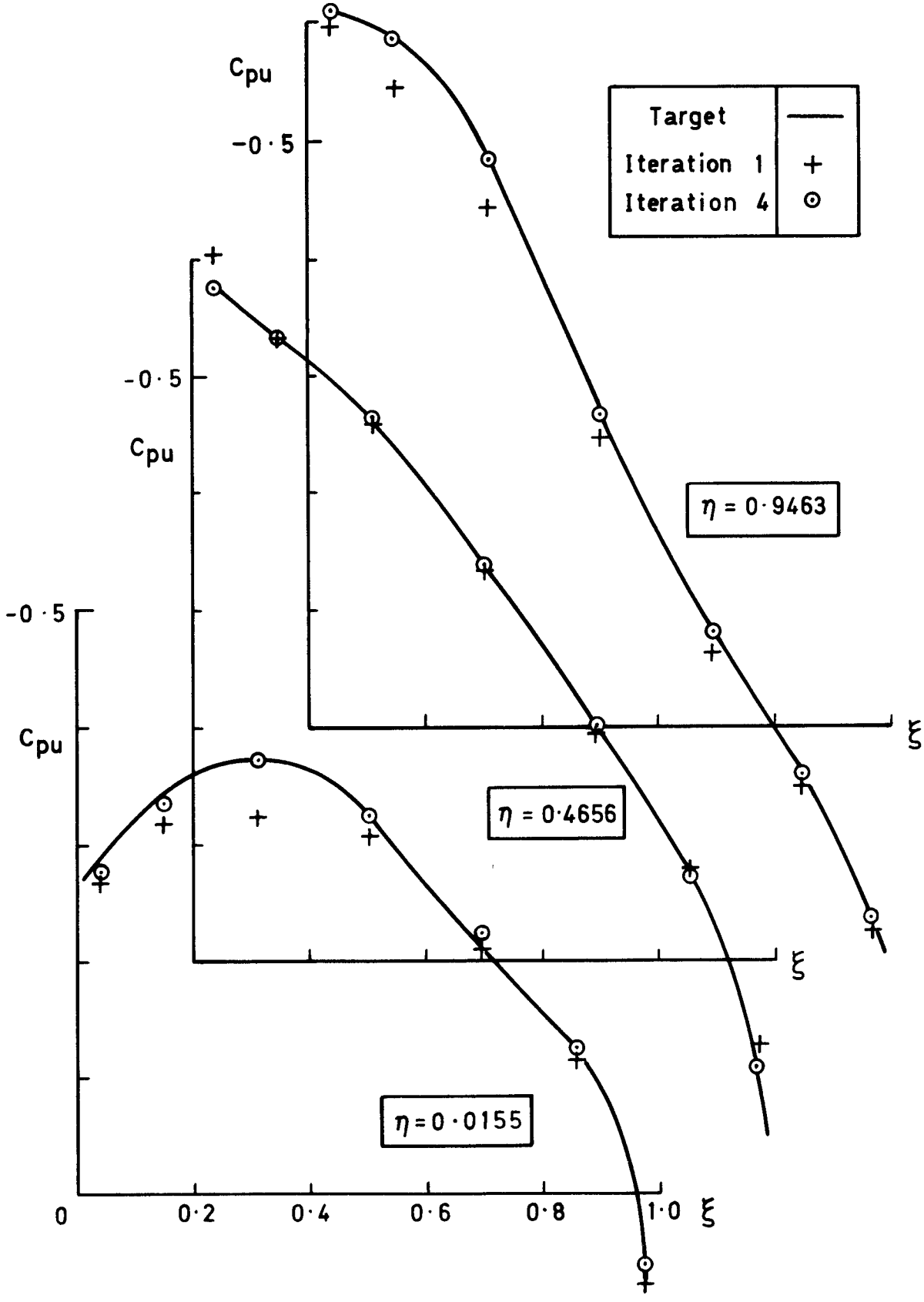

Fig. 7 Iterates for upper-surface pressure distribution on RAE wing "B", $M_\infty = 0 \cdot 8$. Problem 2

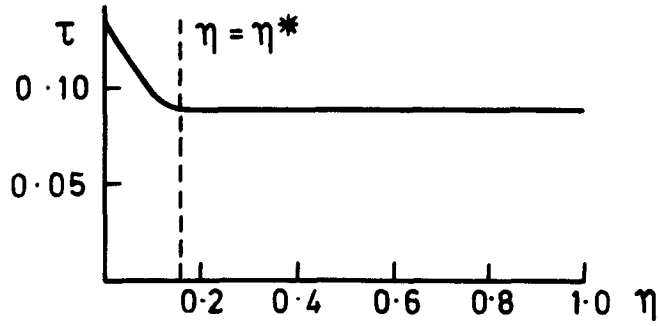

a Spanwise variation of thickness/chord ratio

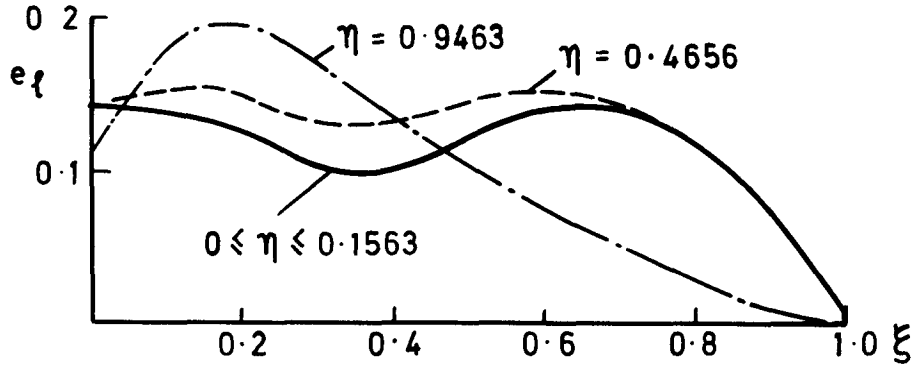

b Design doublet function

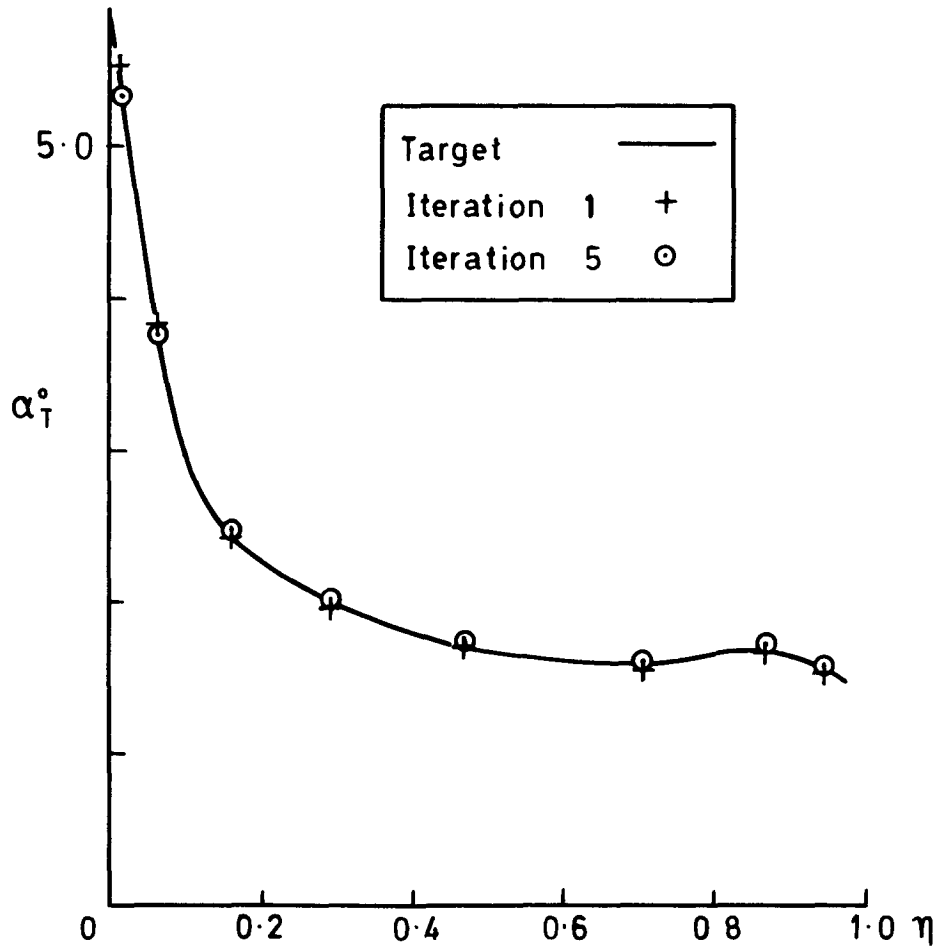

c Iterates for twist distribution

Fig.8a-c Distribution on RAE wing "B," $M_\infty = 0·8$. Problem 3

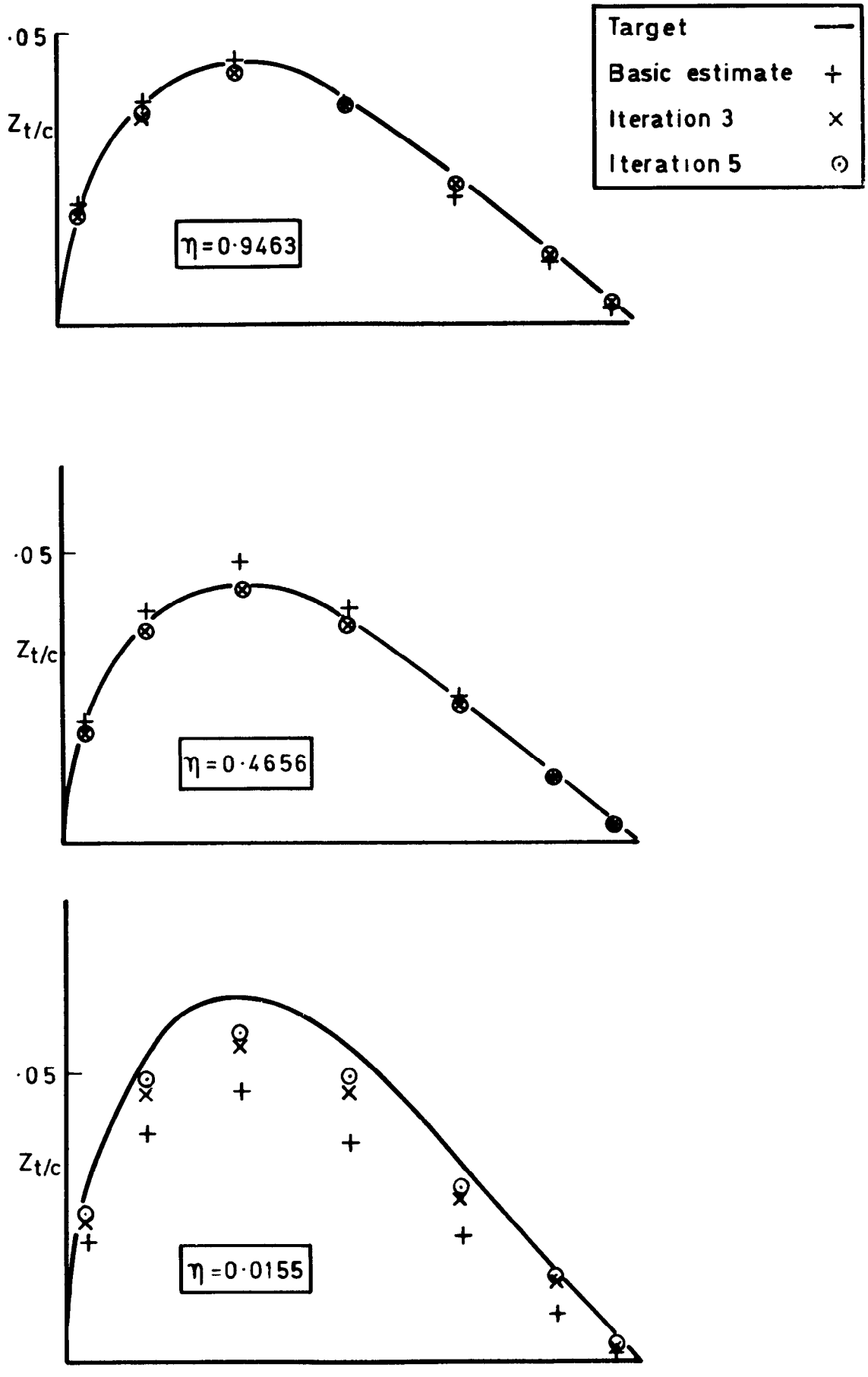

Fig.9 Iterates for thickness distribution on RAE wing "$\hat{B}$", $M_\infty = 0{\cdot}8$. Problem 3

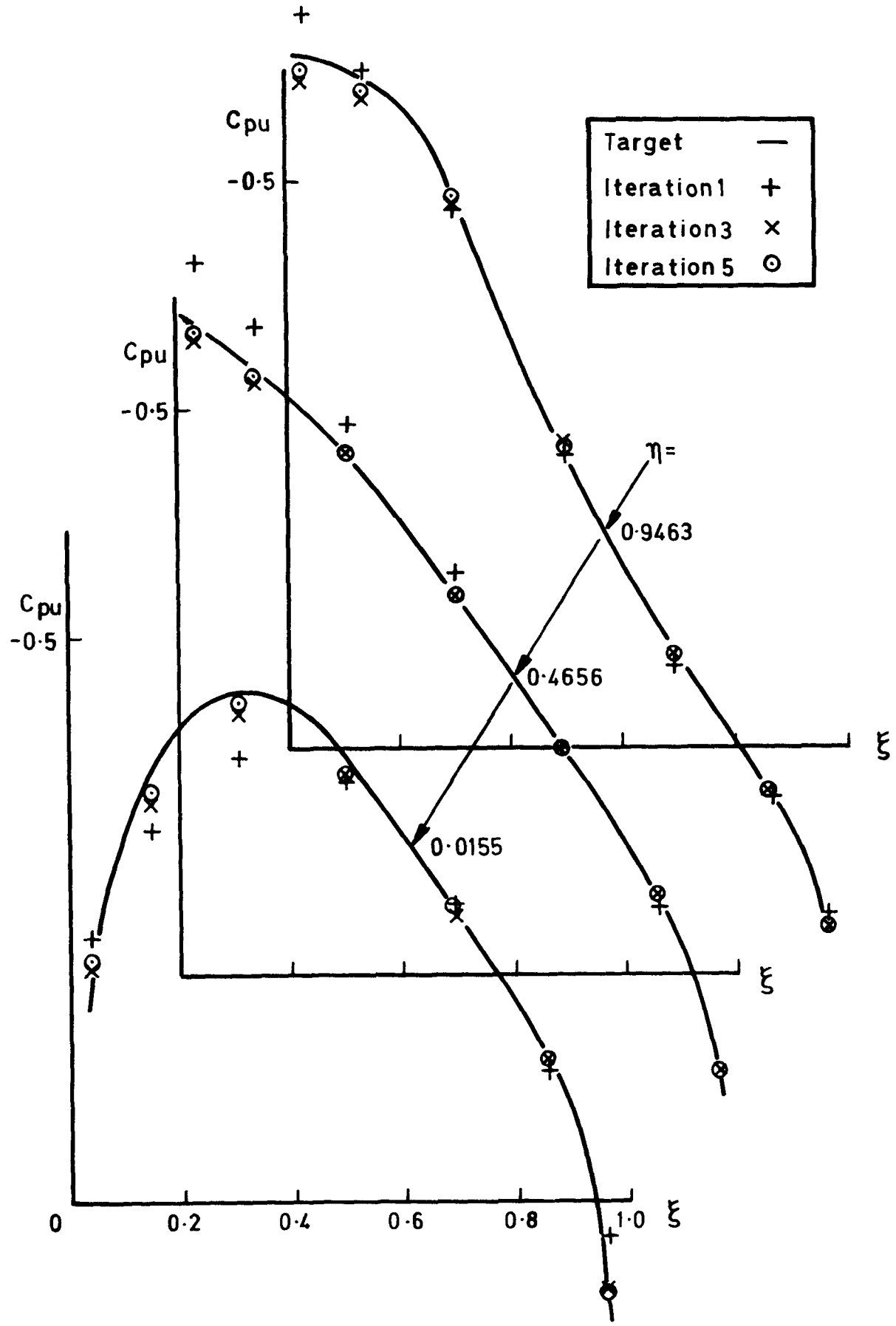

Fig.10 Iterates for upper-surface pressure distribution on RAE wing "$\hat{B}$", M_∞ = 0·8. Problem 3

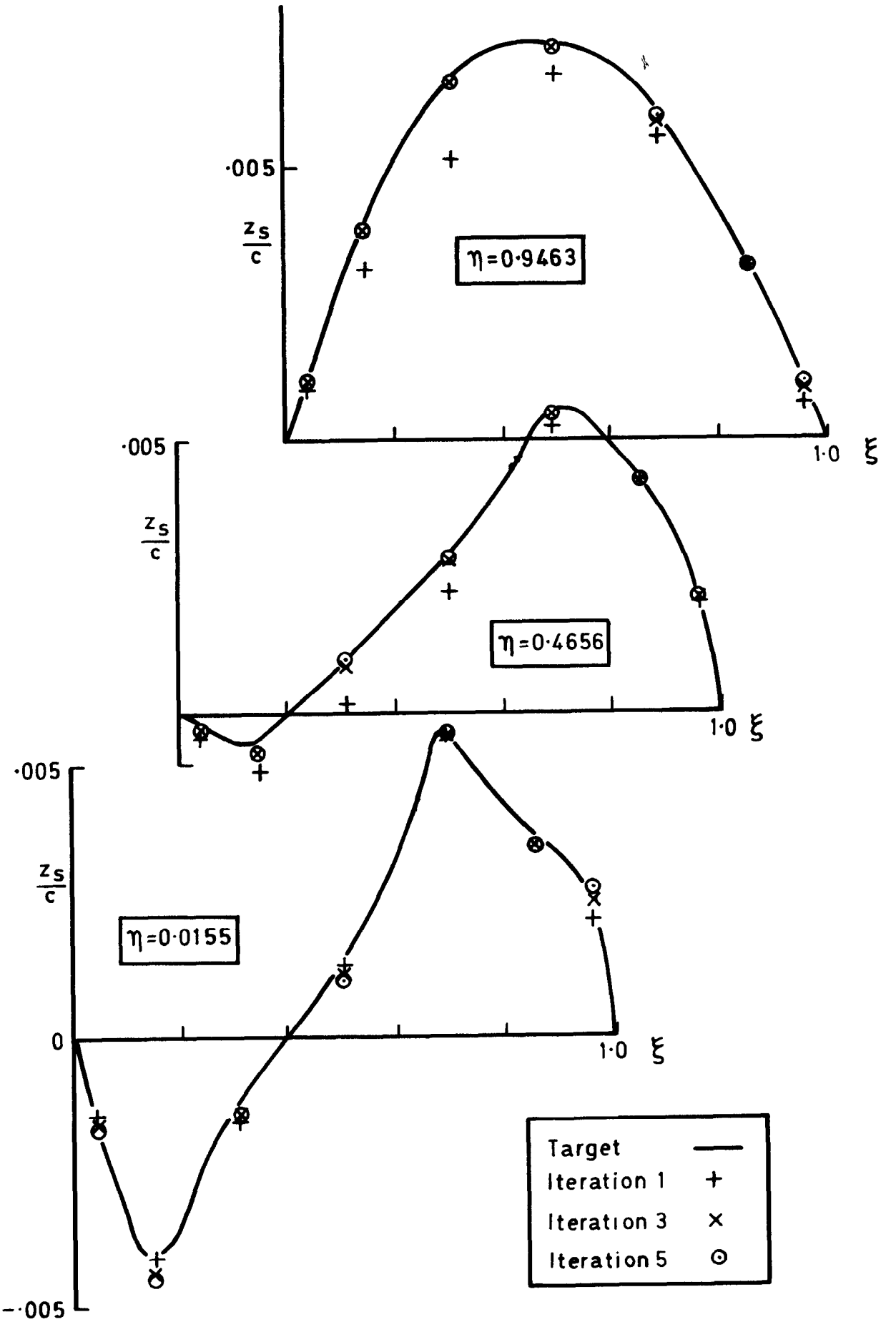

Fig.11 Iterates for camber distribution on RAE wing "$\hat{B}$", M_∞ =0·8. Problem 3

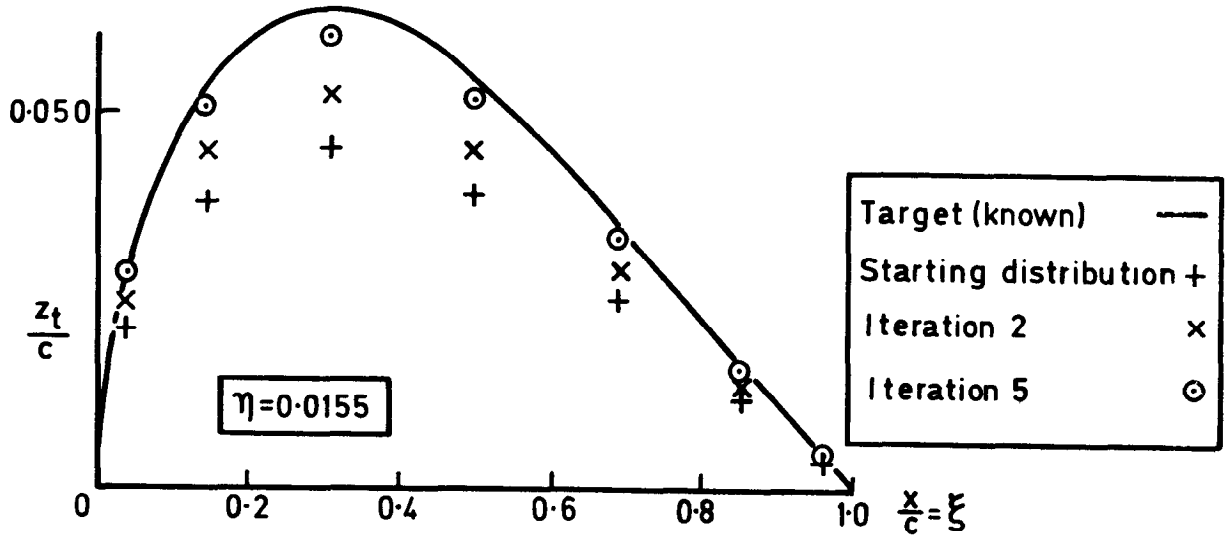

a Thickness distribution near root

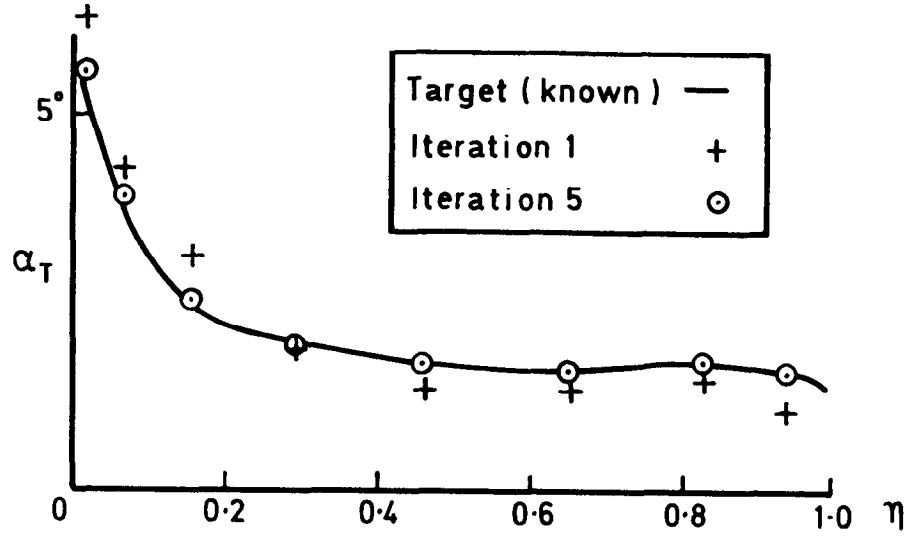

b Twist distribution

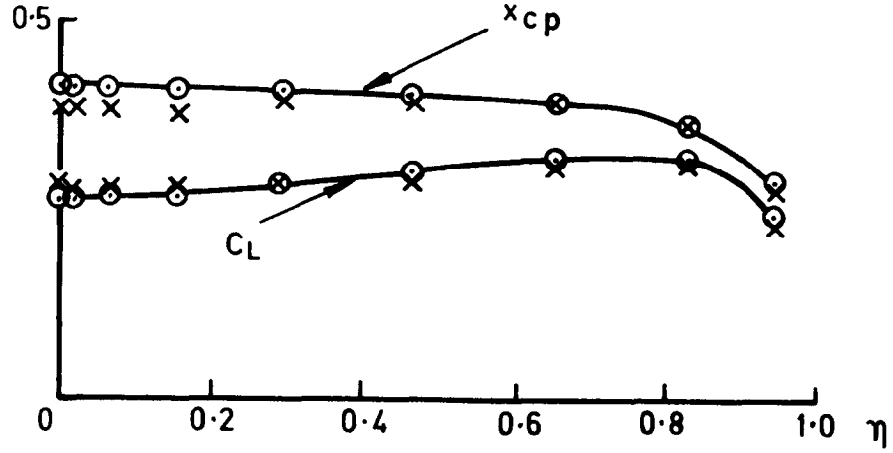

c Section lift and centre of pressure

Fig.12 Iterates for RAE wing "$\hat{B}$", $M_\infty = 0{\cdot}8$. Problem 4

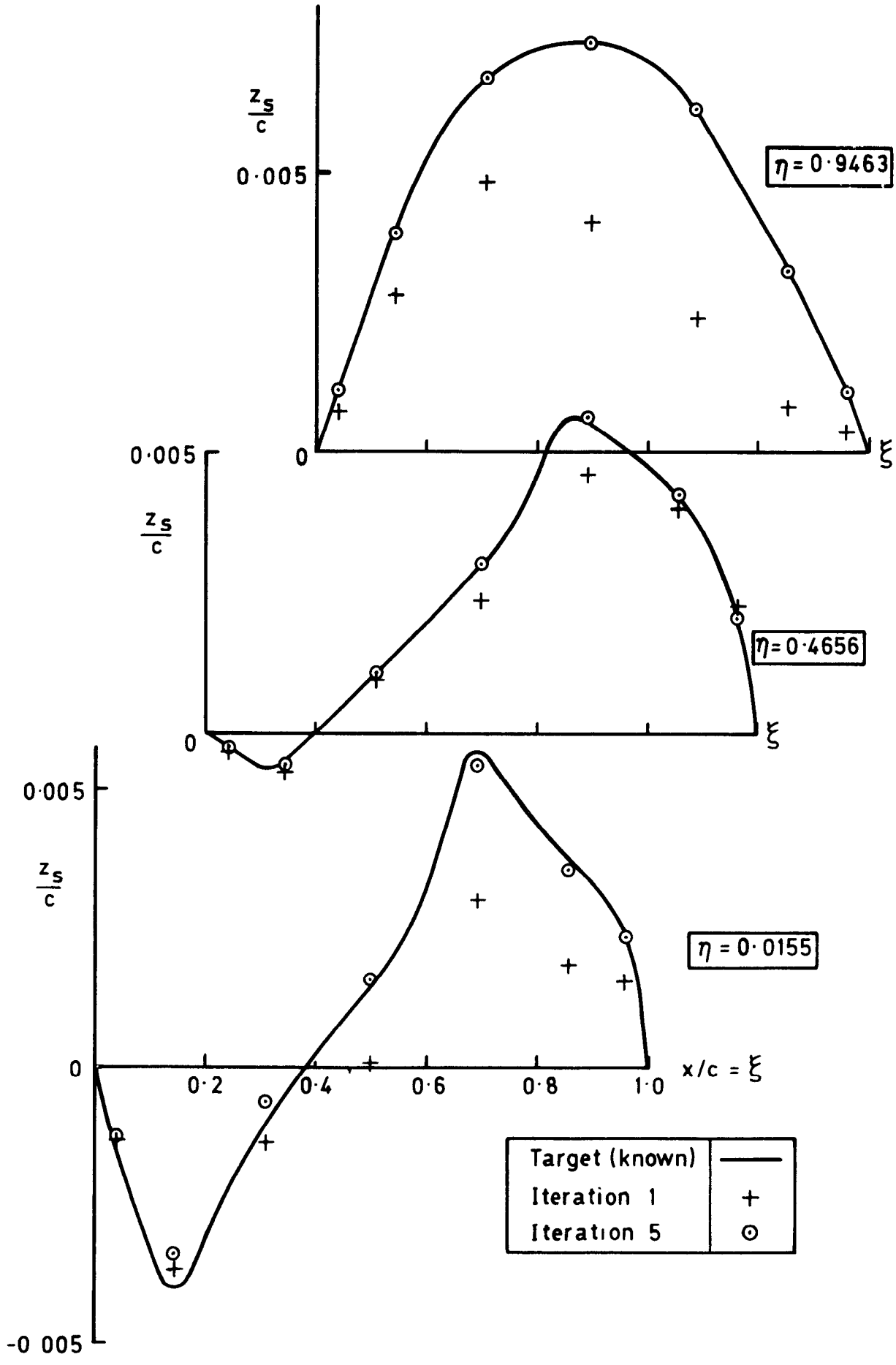

Fig.13 Iterates for camber distribution on RAE wing "$\hat{B}$", $M_\infty = 0 \cdot 8$. Problem 4

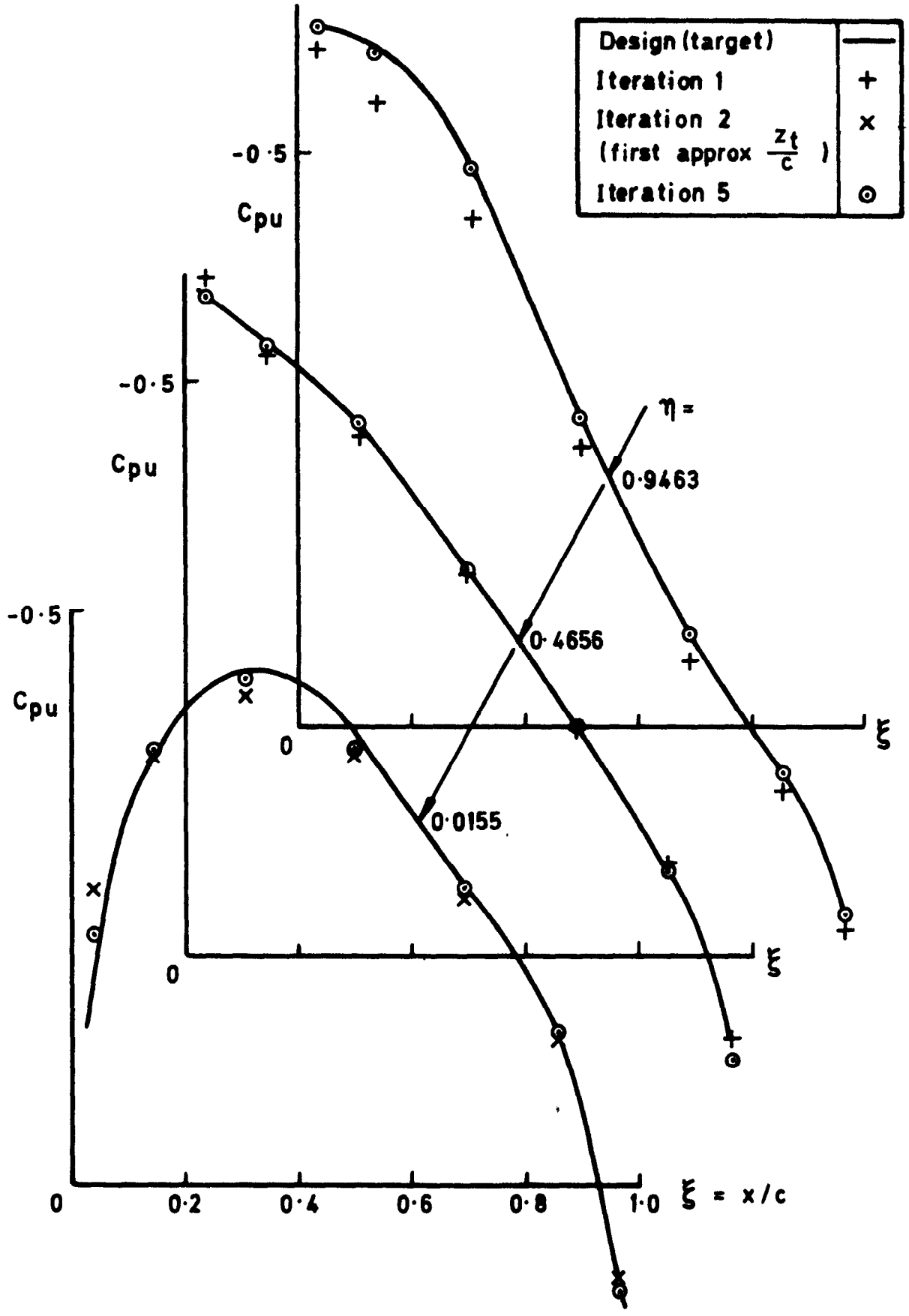

Fig. 14 Iterates for upper-surface pressure distribution on RAE wing "$\hat{B}$", M_∞ = 0·8. Problem 4

Printed in England for Her Majesty's Stationery Office by the Royal Aircraft Establishment, Farnborough Dd. 290279 K5 3/77

ARC CP No.1371
February 1976

Sells, C C L.

533.69.01
533.6.04
533.6.044 7
53..6.043.1
533.6.043 2
533.6 011 32

ITERATIVE DESIGN TECHNIQUES FOR THICK CAMBERED WINGS IN SUBCRITICAL FLOW

The author's method for computing steady, inviscid, subcritical flow past a thick cambered wing is extended to design applications Four problems are considered (1) given thickness and doublet (first-order loading) distributions (2) given thickness and upper-surface pressure distributions (3) given loading and upper-surface pressure distributions, (4) a hybrid of (2) and (3) in which the thickness is specified everywhere except near the root, and is determined near the root when the doublet distribution is constrained to exhibit spanwise invariance in that region. Convergence for the first problem is excellent For all problems, good convergence is obtained outboard For the single case reported of the second problem, convergence was secured near the root but cannot yet be guaranteed. Near the root, slow convergence was obtained for the third problem, rather better convergence for the fourth problem This hybrid option is tentatively recommended

ARC CP No.1371
February 1976

Sells, C C L

533.69.01
533.6.04
533.6.044.7
533.6.043.1
533.6.043.2
533.6.011.32

ITERATIVE DESIGN TECHNIQUES FOR THICK CAMBERED WINGS IN SUBCRITICAL FLOW

The author's method for computing steady, inviscid, subcritical flow past a thick cambered wing is extended to design applications. Four problems are considered: (1) given thickness and doublet (first-order loading) distributions. (2) given thickness and upper-surface pressure distributions, (3) given loading and upper-surface pressure distributions, (4) a hybrid of (2) and (3) in which the thickness is specified everywhere except near the root, and is determined near the root when the doublet distribution is constrained to exhibit spanwise invariance in that region. Convergence for the first problem is excellent. For all problems, good convergence is obtained outboard. For the single case reported of the second problem, convergence was secured near the root but cannot yet be guaranteed Near the root, slow convergence was obtained for the third problem, rather better convergence for the fourth problem This hybrid option is tentatively recommended

Cut here

ARC CP No.1371
February 1976

Sells, C C L

533.69.01
533.6.04
533.6.044 7
533.6.043 1
533.6.043 2
533.6 011 32

ITERATIVE DESIGN TECHNIQUES FOR THICK CAMBERED WINGS IN SUBCRITICAL FLOW

The author's method for computing steady, inviscid, subcritical flow past a thick cambered wing is extended to design applications Four problems are considered (1) given thickness and doublet (first-order loading) distributions, (2) given thickness and upper-surface pressure distributions, (3) given loading and upper-surface pressure distributions, (4) a hybrid of (2) and (3) in which the thickness is specified everywhere except near the root, and is determined near the root when the doublet distribution is constrained to exhibit spanwise invariance in that region Convergence for the first problem is excellent For all problems, good convergence is obtained outboard For the single case reported of the second problem convergence was secured near the root but cannot yet be guaranteed Near the root, slow convergence was obtained for the third problem, rather better convergence for the fourth problem This hybrid option is tentatively recommended

Cut here

DETACHABLE ABSTRACT CARDS

DETACHABLE ABSTRACT CARDS

Published by
HER MAJESTY'S STATIONERY OFFICE

Government Bookshops
49 High Holborn, London WC1V 6HB
13a Castle Street, Edinburgh EH2 3AR
41 The Hayes, Cardiff CF1 1JW
Brazennose Street, Manchester M60 8AS
Southey House, Wine Street, Bristol BS1 2BQ
258 Broad Street, Birmingham B1 2HE
80 Chichester Street, Belfast BT1 4JY

Government Publications are also available through booksellers

C.P. No. 1371

ISBN 011 471117 8